

Supporting Information for:

Nitric Oxide Release from a Nickel Nitrosyl Complex Induced by One Electron Oxidation

Ashley M. Wright, Homaira T. Zaman, Guang Wu, Trevor W. Hayton*

Department of Chemistry and Biochemistry, University of California Santa Barbara, Santa

Barbara CA 93106

*To whom correspondence should be addressed. Email: hayton@chem.ucsb.edu

Table of Contents

Experimental Details.....	S3
NMR spectroscopy	S6
IR and UV-vis Spectra.....	S16
Gas Chromatography	S24
Reactivity Studies	S26
Electrochemistry	S36
References.....	S40

Experimental Details

Oxidation of 2 with [Cp₂Fe][PF₆]. An NMR tube was charged with [Ni(NO)(bipy)][PF₆] (21 mg, 0.054 mmol) and CD₂Cl₂ (0.5 mL) and an initial NMR spectrum was recorded. [Cp₂Fe][PF₆] (19 mg, 0.059 mmol) was added as a CD₂Cl₂ solution (0.5 mL). The reaction was monitored by ¹H NMR spectroscopy for 8 h. No reaction was observed over this time frame (see Figure S33).

Addition of MeCN to 2. An NMR tube was charged with [Ni(NO)(bipy)][PF₆] (**2**) (23 mg, 0.059 mmol) and CD₂Cl₂ (0.7 mL) and an initial NMR spectrum was recorded. ¹H NMR (CD₂Cl₂, 22 °C, 400 MHz): δ 7.88 (2H), 7.94 (2H), 8.15 (2H), 10.23 (2H). ¹⁹F NMR (CD₂Cl₂, 22 °C, 376 MHz): δ -69.68 (d, J_{PF} = 651 Hz, FWHM = 1150 Hz). ³¹P NMR (CD₂Cl₂, 22 °C, 170 MHz): δ -139.8 (br sept, J_{PF} = 785 Hz, FWHM = 1040 Hz). Acetonitrile (15 μL, 0.29 mmol, 5.3 eq) was then transferred via microsyringe to the NMR tube. An immediate color change from green to deep violet was observed. An NMR spectrum of this sample reveals signals assignable to a new species, tentatively formulated as [Ni(NO)(bipy)(MeCN)][PF₆] (see Figure S13 and S14). ¹H NMR (CD₂Cl₂, 22 °C, 400 MHz): δ 1.99 (MeCN), 7.90 (2H, bipy), 8.20 (4H, bipy), 10.15 (2H, bipy). ¹⁹F NMR (CD₂Cl₂, 22 °C, 376 MHz): δ -73.22 (d, J_{PF} = 710 Hz, FWHM = 2.26 Hz); ³¹P NMR (CD₂Cl₂, 22 °C, 170 MHz): δ -144.52 (br sept, J_{PF} = 702 Hz, FWHM = 4.25 Hz).

Thermolysis of [Ni(NO)(bipy)][PF₆]. An air-free NMR tube was charged with [Ni(NO)(bipy)][PF₆] (**2**) (25 mg, 0.064 mmol) and CD₃NO₂ (0.5 mL). An initial NMR spectrum was recorded. The solution was then heated at 90 °C for 21 h. No color change was observed. The ¹H NMR spectrum was recorded again and revealed only a slight broadening of the signals associated with **2**. In addition, minor resonances assignable to the formation of several

paramagnetic products, including $[\text{Ni}(\text{bipy})_3]^{2+}$, were also present in the spectrum (see Figure S36 and S37).

Thermolysis of $[\{\text{Ni}(\text{NO})(\text{bipy})\}_2(\mu\text{-S}_2\text{Ph}_2)][\text{PF}_6]_2$ (3**).** A J-Young type NMR tube was charged with $[\{\text{Ni}(\text{NO})(\text{bipy})\}_2(\mu\text{-S}_2\text{Ph}_2)][\text{PF}_6]_2$ (23 mg, 0.023 mmol) and $1,1,2,2\text{-C}_2\text{Cl}_4\text{D}_2$ (0.7 mL). The reaction mixture was heated at 60 °C for 24 h and the reaction was periodically monitored by ^1H NMR spectroscopy. A green precipitate was generated over the course of the reaction and the solution was a pale green in color. After 24 h, there were only weak and broad signals in the ^1H NMR spectrum (see Figure S38).

Oxidation of **2 with TEMPO.** *NMR spectroscopy.* An NMR tube was charged with $[\text{Ni}(\text{NO})(\text{bipy})][\text{PF}_6]$ (32 mg, 0.081 mmol) and CD_2Cl_2 (0.7 mL). TEMPO (15 mg, 0.097 mmol, 1.2 equiv) was then added to the mixture. Immediate gas evolution was observed and the solution transformed to an orange brown color. The ^1H NMR spectrum was recorded, revealing the quantitative formation of $[\text{Ni}(\text{bipy})(\text{TEMPO})][\text{PF}_6]$ (see Figure S32).

Nitric Oxide Analyzer. Stock solutions of $[\text{Ni}(\text{NO})(\text{bipy})][\text{PF}_6]$ and TEMPO in CH_2Cl_2 were prepared with concentrations of 3.85 mM and 19.5 mM, respectively. An aliquot of the $[\text{Ni}(\text{NO})(\text{bipy})][\text{PF}_6]$ solution (0.50 mL, 1.92×10^{-6} mol) was transferred via syringe to a gas tight reaction flask. Subsequently, TEMPO (0.15 mL, 2.92×10^{-6} mol) was injected through a rubber septum in to the reaction flask. Gas evolution occurred immediately and the green solution transformed to an orange brown color. A 2 μL volume of the head space was sampled using a gas tight syringe and injected into the Nitric Oxide Analyzer. The area of the peak was compared to a calibration curve and the amount of NO formation was determined to be 59% (average based on three injections).

Reaction of 2 with TEMPO in the presence of MeCN. A CD₂Cl₂ solution of (0.7 mL) [Ni(NO)(bipy)][PF₆] (**2**) (23 mg, 0.059 mmol) and acetonitrile (15 μL, 0.29 mmol, 5.3 eq) was transferred to a 20 mL scintillation vial containing crystalline TEMPO (10.7 mg, 0.068 mmol, 1.15 eq) and stirred vigorously. The solution immediately transformed from a deep purple color to dark blue-green. The reaction was monitored over 24 h by ¹H NMR spectroscopy. After 24 h, signals attributable to complex **4** were observed; however, only ~28% of complex **2** had reacted with TEMPO (see Figure S34).

Addition of TEMPO to (bipy)Ni(NO)(I) (1). TEMPO (26 mg, 0.16 mmol) was added to a suspension of (bipy)Ni(NO)(I) (36 mg, 0.098 mmol) in CH₂Cl₂ (5 mL). The reaction was monitored by solution IR spectroscopy for 24 hours. No change in the NO stretching frequency of **1** was observed over this time.

NMR spectroscopy

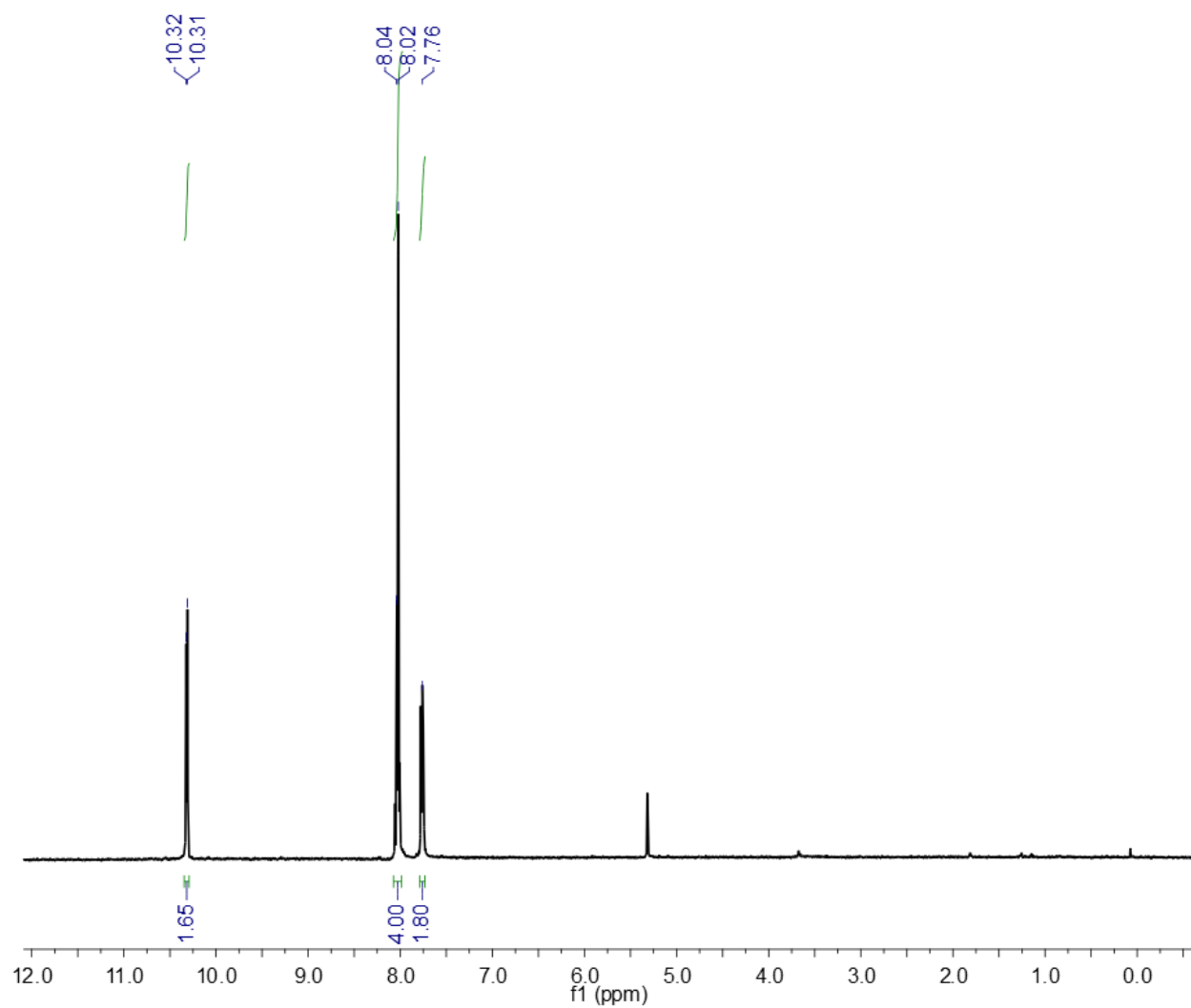


Figure S1. ^1H NMR spectrum (CD_2Cl_2 , 22 °C, 400 MHz) of (bipy)Ni(NO)(I) (**1**).

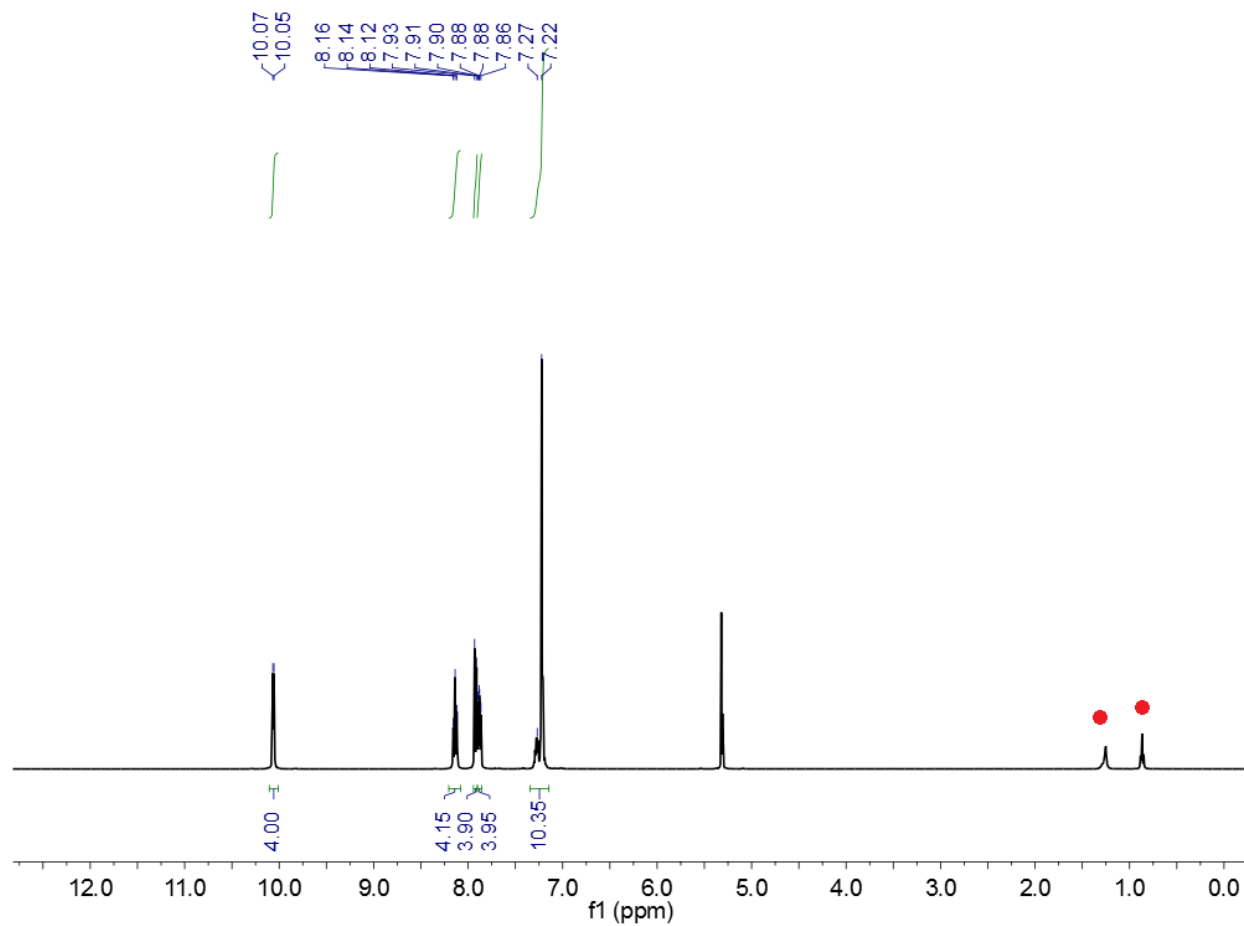


Figure S2. ¹H NMR spectrum (CD₂Cl₂, 22 °C, 400 MHz) of [{(NO)(bipy)Ni}₂(μ-S₂Ph₂)] [PF₆]₂ (3). The red circle (●) denotes a hexane impurity.

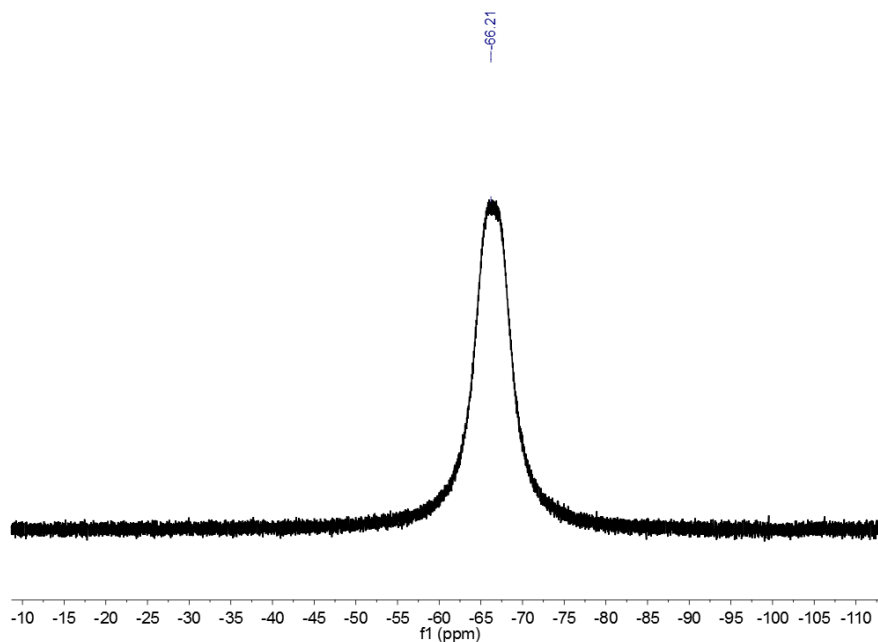


Figure S3. ^{19}F NMR spectrum (CD_2Cl_2 , 22 °C, 376 MHz) of $[\{(\text{NO})(\text{bipy})\text{Ni}\}_2(\mu\text{-S}_2\text{Ph}_2)][\text{PF}_6]_2$ (**3**).

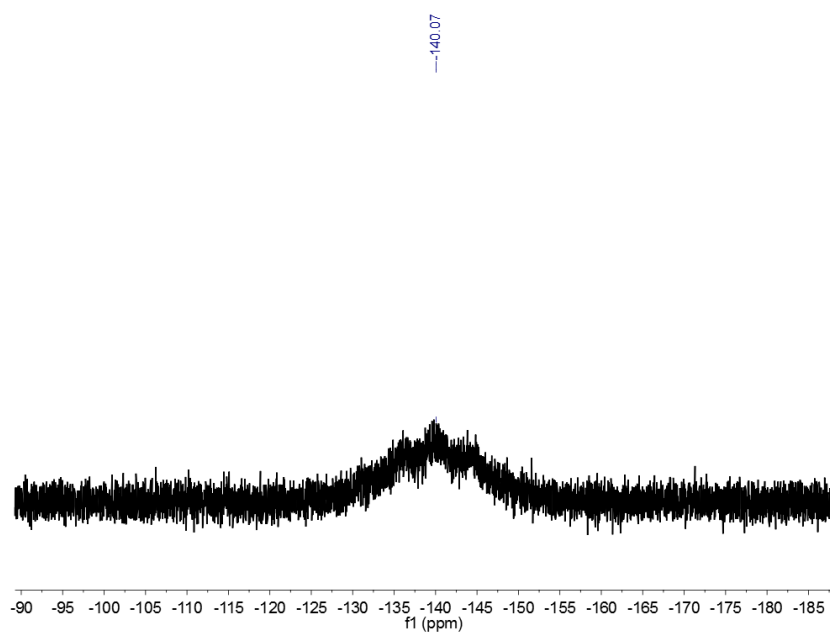


Figure S4. $^{31}\text{P}\{^1\text{H}\}$ NMR spectrum (CD_2Cl_2 , 22 °C, 170 MHz) of $[\{(\text{NO})(\text{bipy})\text{Ni}\}_2(\mu\text{-S}_2\text{Ph}_2)][\text{PF}_6]_2$ (**3**).

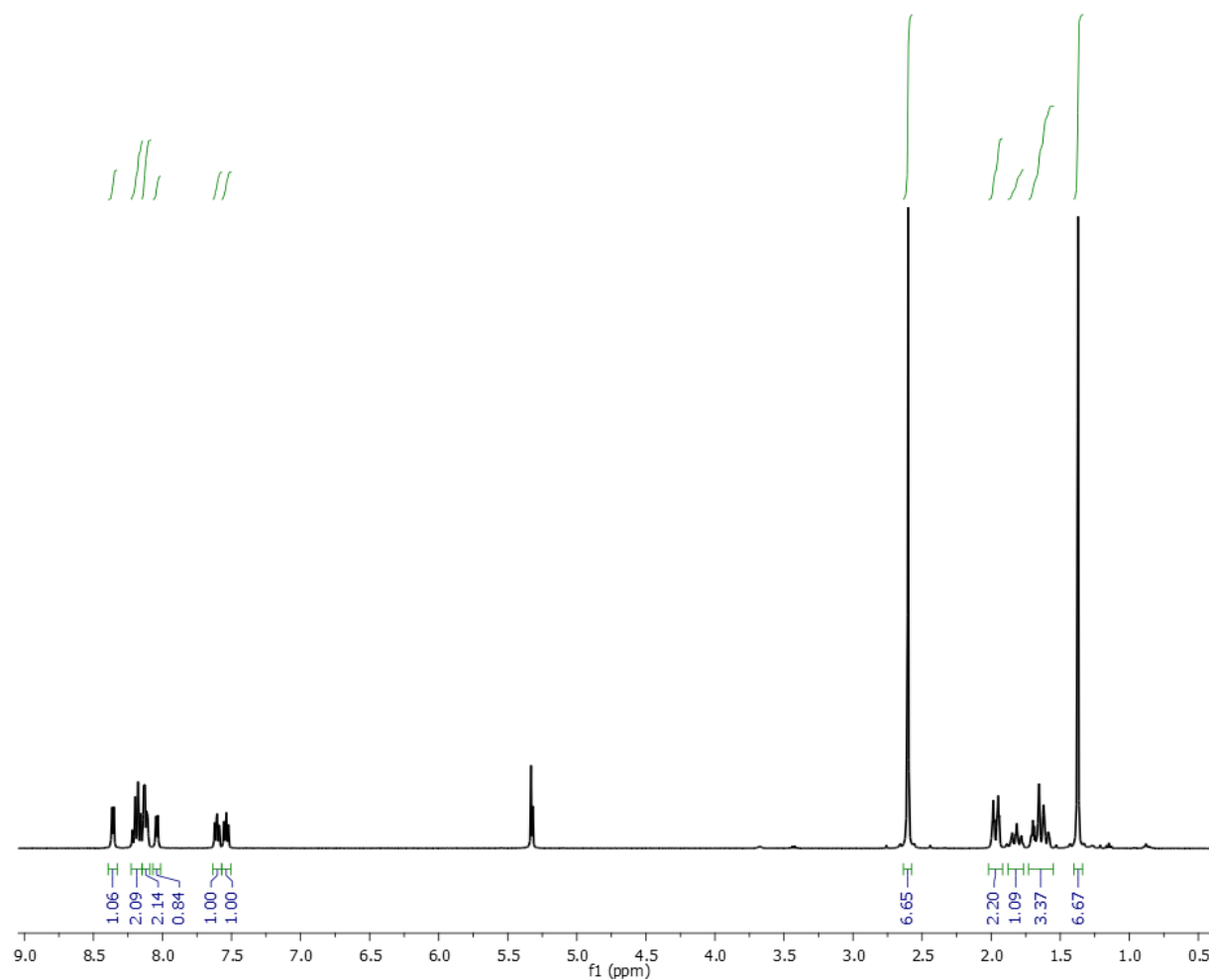


Figure S5. ^1H NMR spectrum (CD_2Cl_2 , 22°C , 400 MHz) of $[\text{Ni}(\text{bipy})(\eta^2\text{-TEMPO})][\text{PF}_6]$ (**4**).

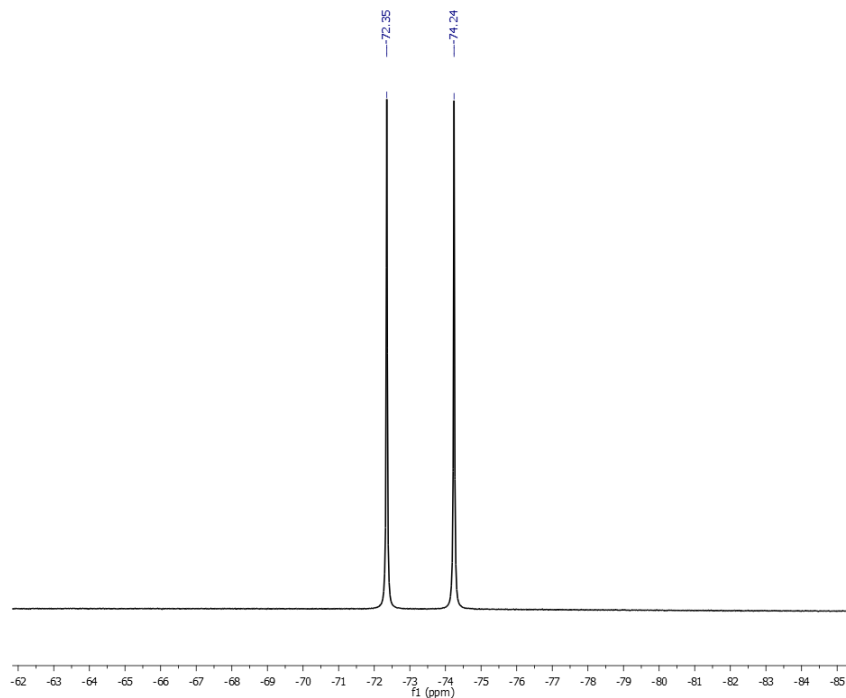


Figure S6. ^{19}F NMR spectrum (CD_2Cl_2 , 22 °C, 376 MHz) of $[\text{Ni}(\text{bipy})(\eta^2\text{-TEMPO})][\text{PF}_6]$ (**4**).

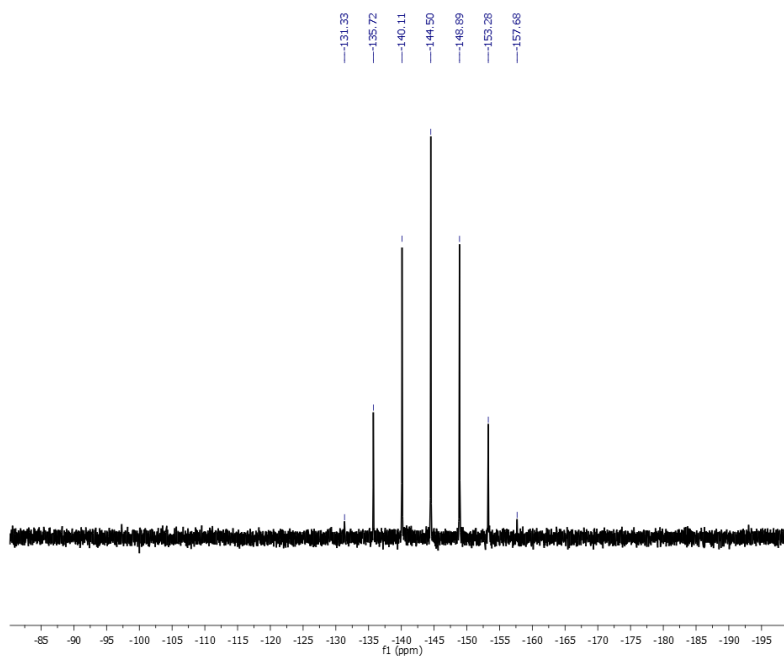


Figure S7. $^{31}\text{P}\{^1\text{H}\}$ NMR spectrum (CD_2Cl_2 , 22 °C, 170 MHz) of $[\text{Ni}(\text{bipy})(\eta^2\text{-TEMPO})][\text{PF}_6]$ (**4**).

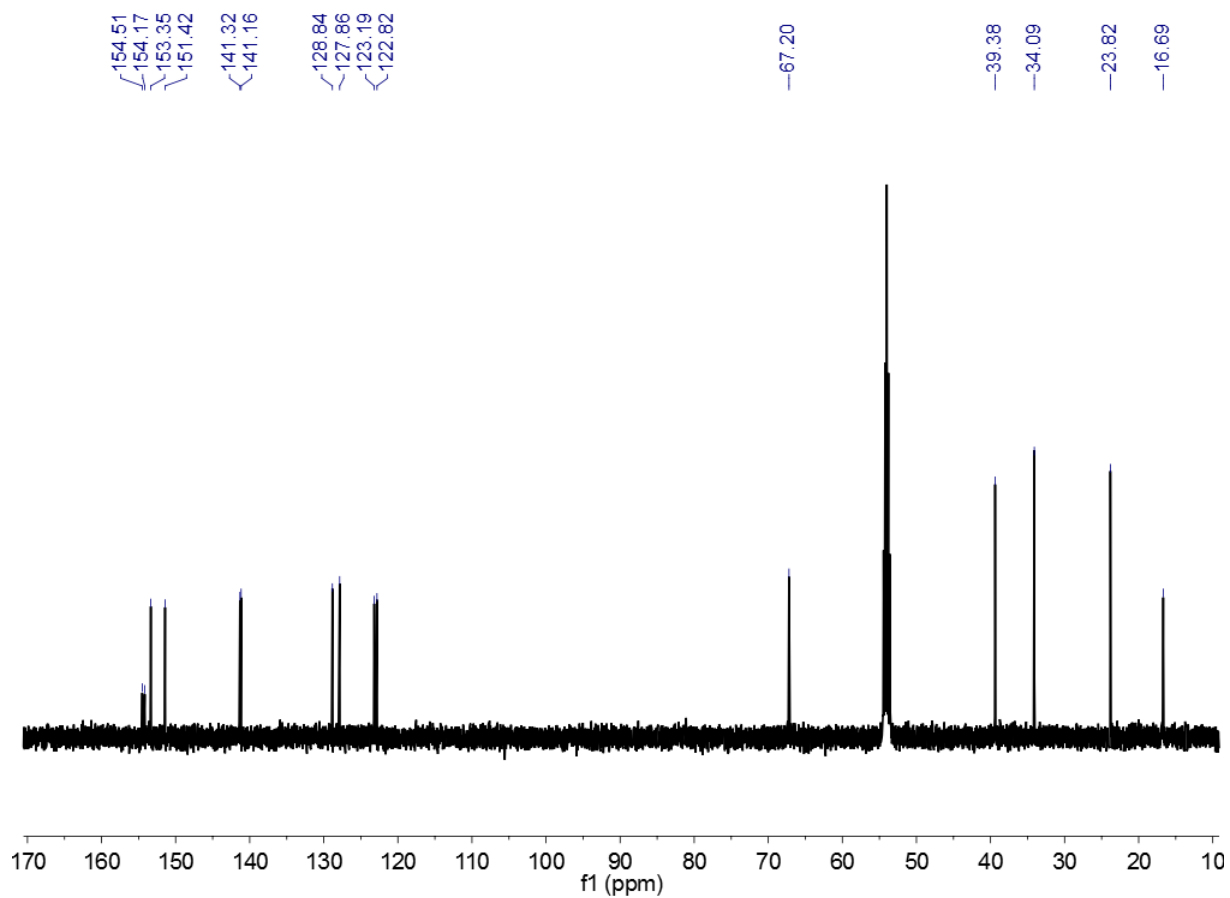


Figure S8. ^{13}C NMR spectrum (CD_2Cl_2 , 22 °C, 125 MHz) of $[\text{Ni}(\text{bipy})(\eta^2\text{-TEMPO})][\text{PF}_6]$ (**4**).

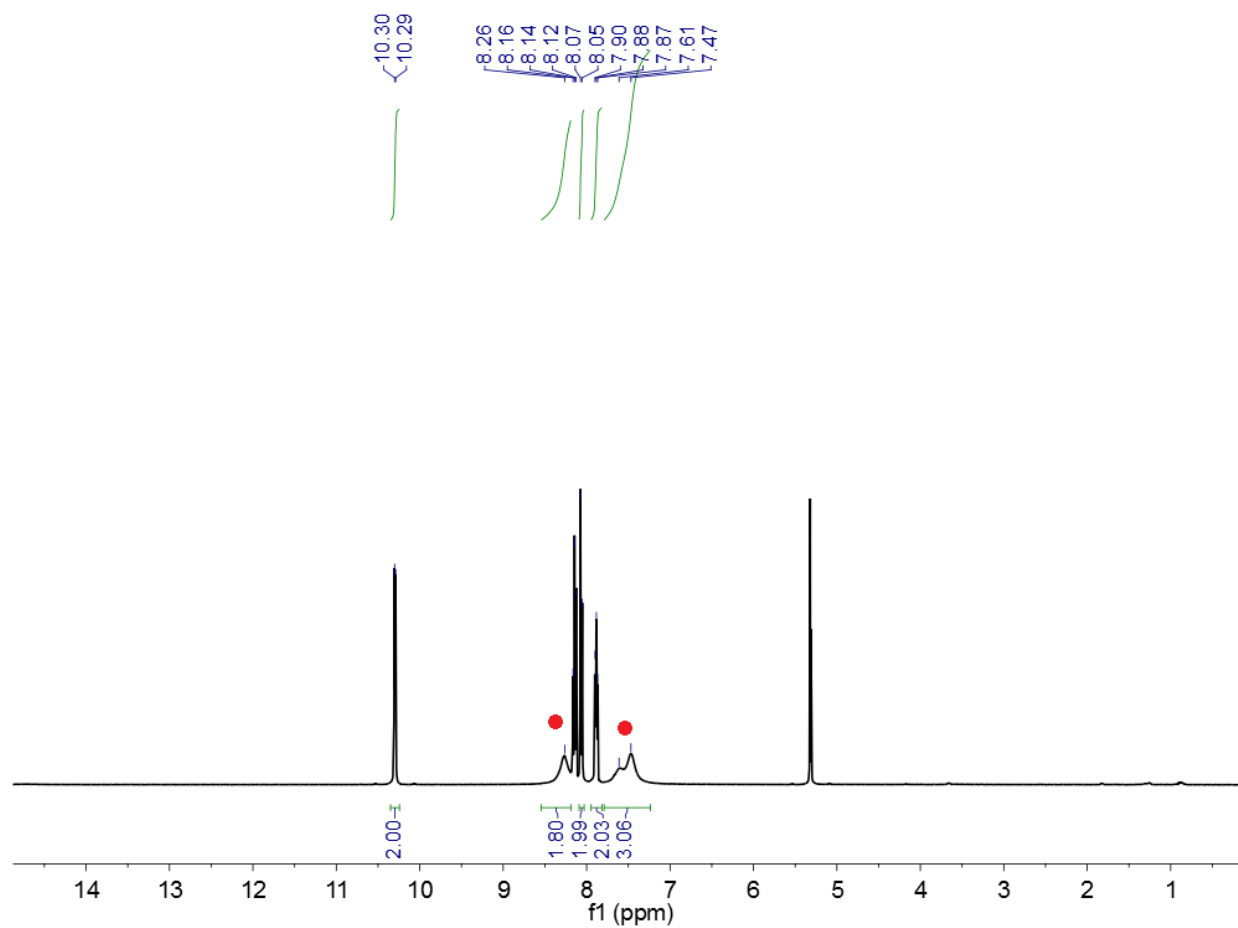


Figure S9. ^1H NMR spectrum (CD_2Cl_2 , 400 MHz, 22 $^\circ\text{C}$) of $[(\text{bipy})\text{NiNO}(\text{ONC}_5\text{H}_5)][\text{PF}_6]$ (5).

The red circles (●) denote the aryl resonances of pyridine.

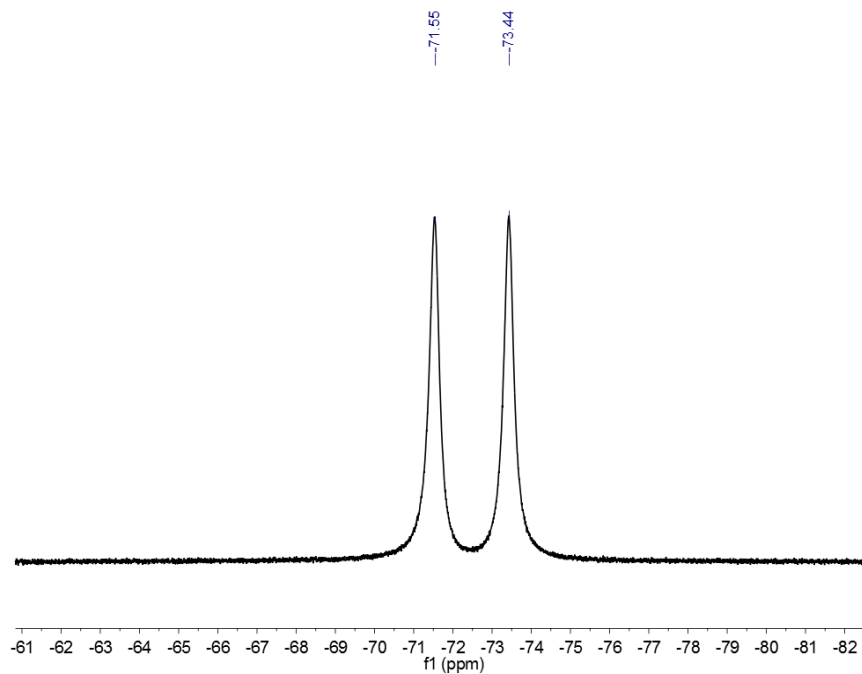


Figure S10. ^{19}F NMR spectrum (CD_2Cl_2 , 376 MHz, 22 °C) of $[(\text{bipy})\text{NiNO}(\text{ONC}_5\text{H}_5)][\text{PF}_6]$ (**5**).

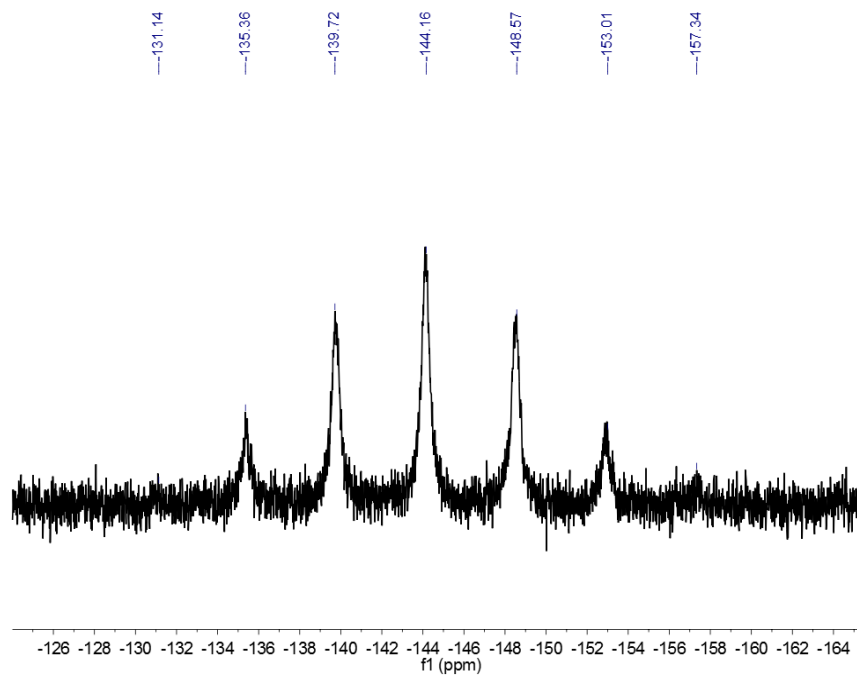


Figure S11. $^{31}\text{P}\{^1\text{H}\}$ NMR spectrum (CD_2Cl_2 , 170 MHz, 22 °C) of $[(\text{bipy})\text{NiNO}(\text{ONC}_5\text{H}_5)][\text{PF}_6]$ (**5**).

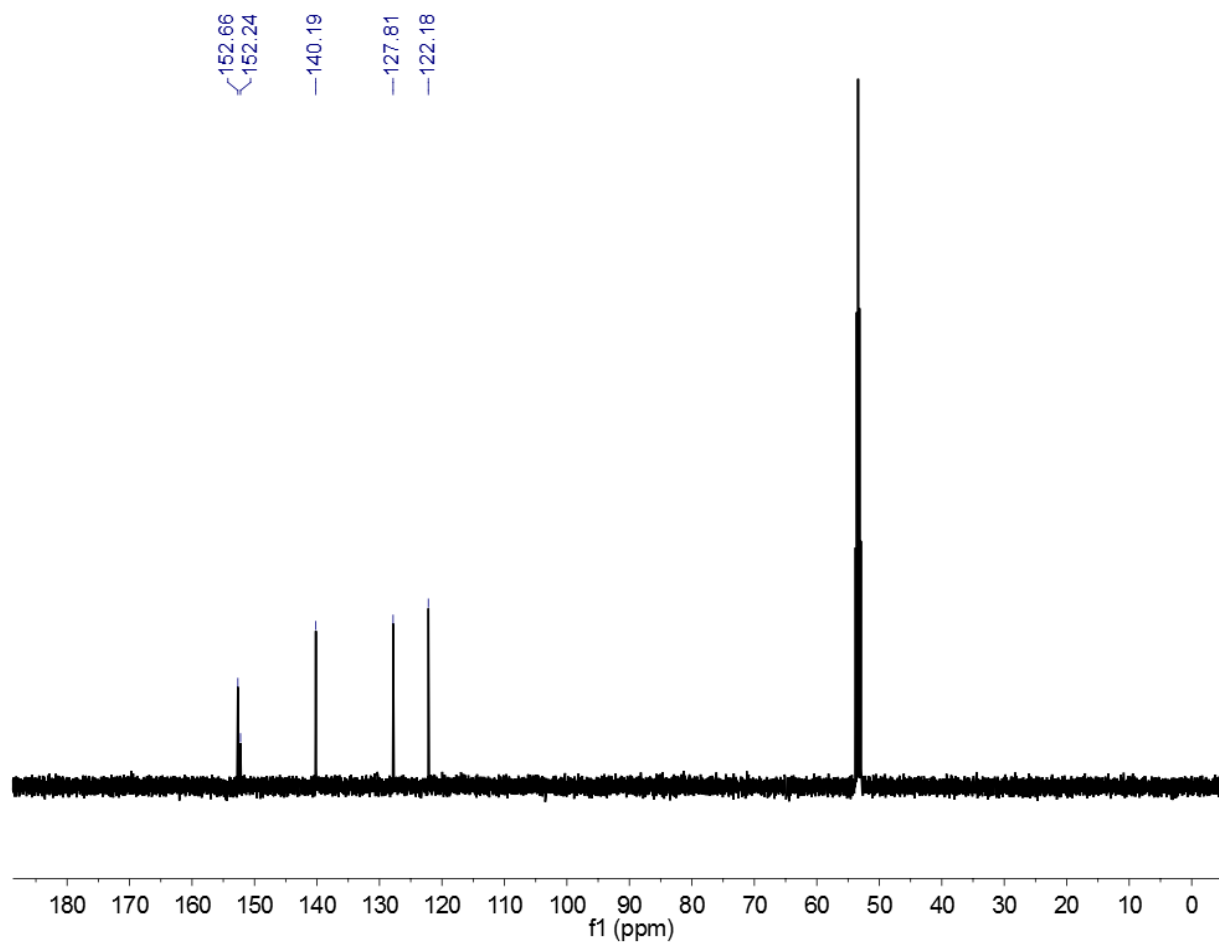


Figure S12. ^{13}C NMR spectrum (CD_2Cl_2 , 22 °C, 125 MHz) of $[(\text{bipy})\text{NiNO}(\text{ONC}_5\text{H}_5)][\text{PF}_6]$ (**5**).

At room temperature the signals for the ONC_5H_5 are not observed.

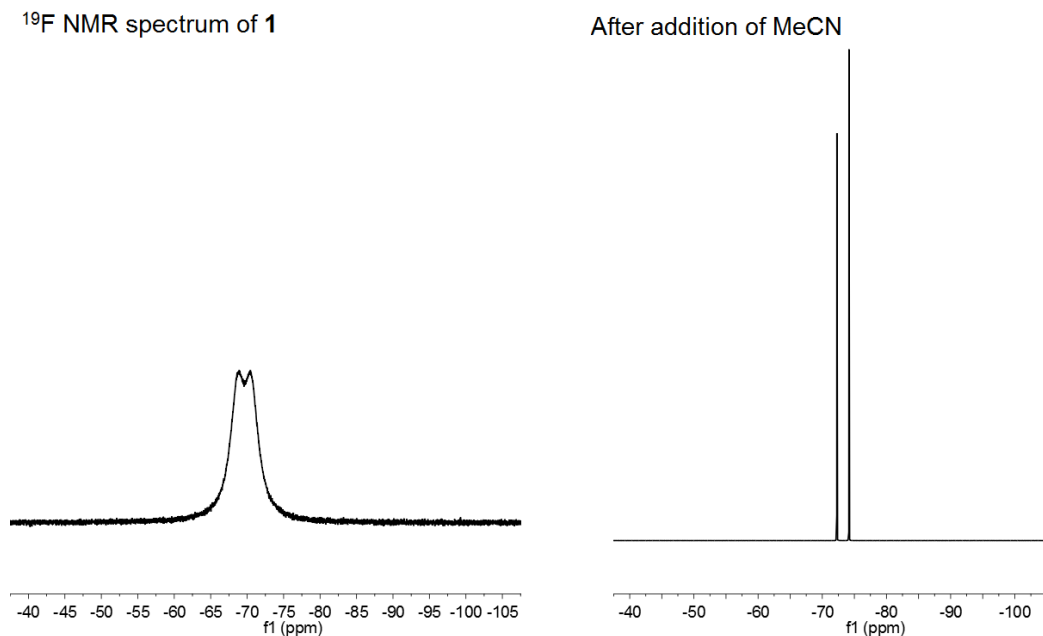


Figure S13. ^{19}F NMR spectrum (CD_2Cl_2 , 376 MHz, 22 °C) of $[\text{Ni}(\text{NO})(\text{bipy})][\text{PF}_6]$ before (*left* spectrum) and after (*right* spectrum) addition of 5 equiv of MeCN.

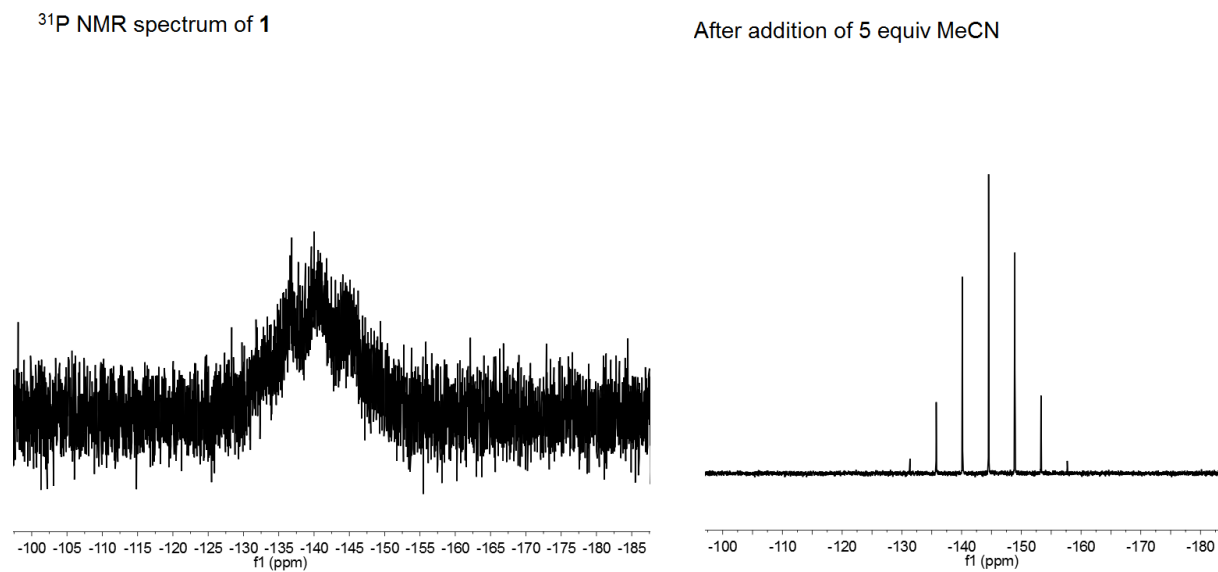


Figure S14. $^{31}\text{P}\{^1\text{H}\}$ NMR spectrum (CD_2Cl_2 , 176 MHz, 22 °C) of $[\text{Ni}(\text{NO})(\text{bipy})][\text{PF}_6]$ before (*left* spectrum) and after (*right* spectrum) addition of 5 equiv of MeCN.

IR and UV-vis Spectra

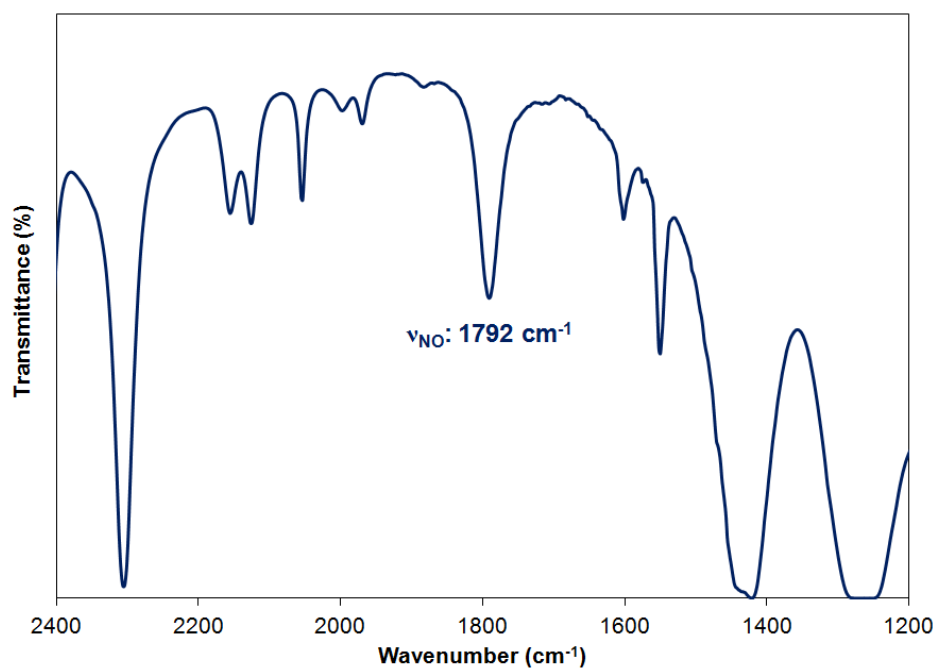


Figure S15. Solution IR spectrum (CH₂Cl₂, 25 °C) of (bipy)Ni(NO)(I) (**1**).

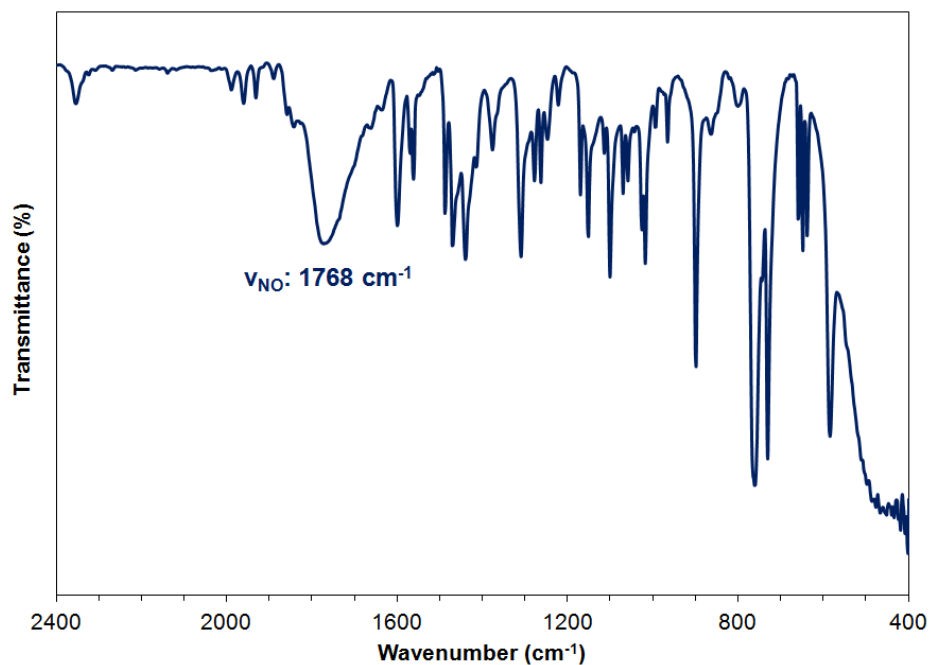


Figure S16. Solid State IR spectrum (Nujol mull) of (bipy)Ni(NO)(I) (**1**).

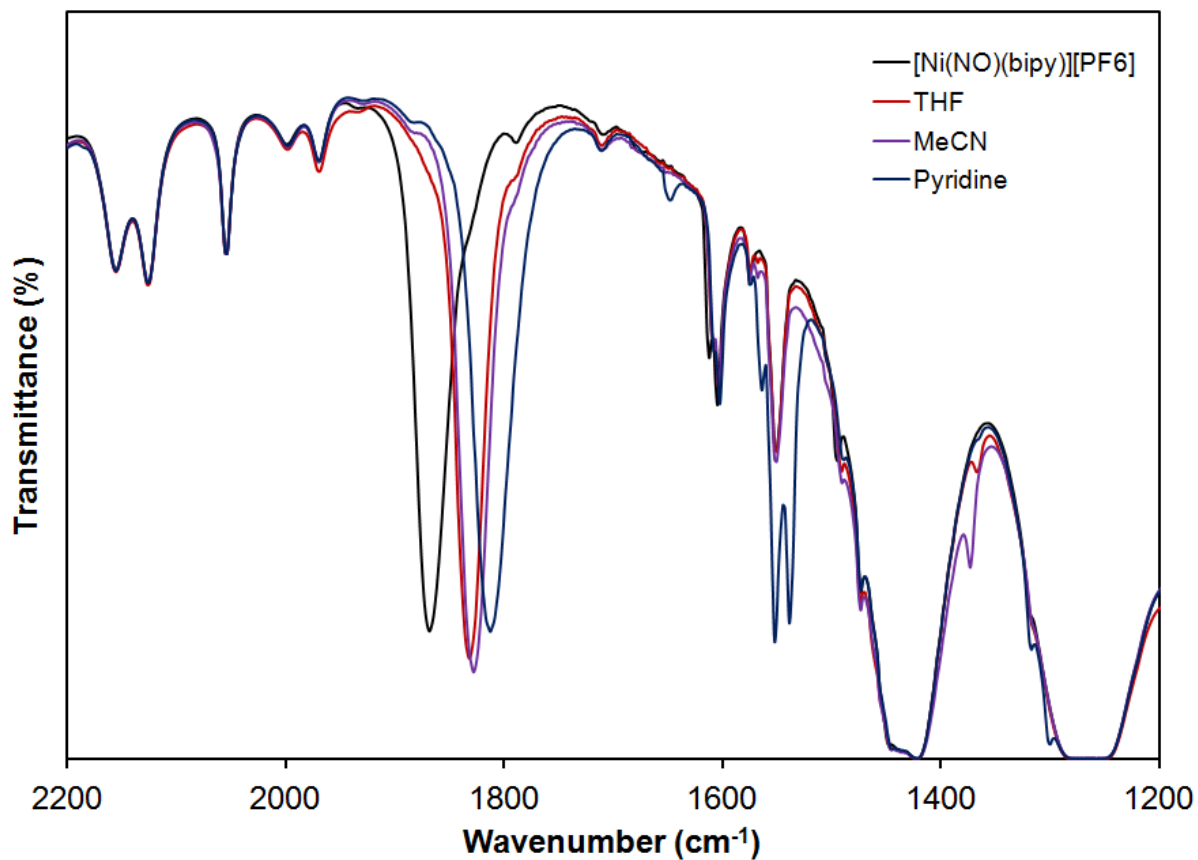


Figure S17. Solution phase IR spectra of $[\text{Ni}(\text{NO})(\text{bipy})(\text{L})][\text{PF}_6]$ in CH_2Cl_2 (L = THF, py, MeCN).

Table S1. NO stretching frequencies of $[\text{Ni}(\text{NO})(\text{bipy})(\text{L})][\text{PF}_6]$.

Ligand (L)	NO stretching frequency (cm^{-1})	Guttman Donor Number ¹
none	1868	-
THF	1832	20.0
MeCN	1828	14.1
py	1813	33.1

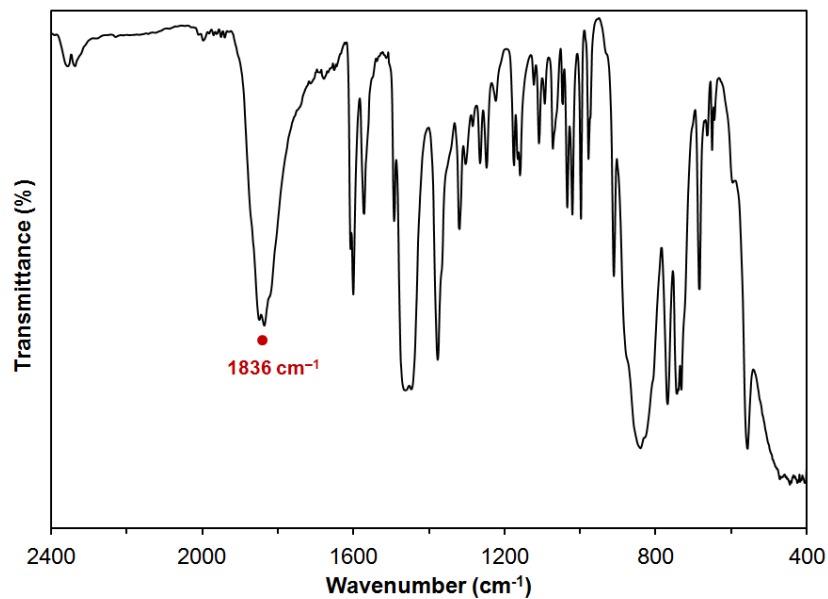


Figure S18. Solid state IR spectrum (Nujol mull) of $[\{(\text{NO})(\text{bipy})\text{Ni}\}_2(\mu\text{-S}_2\text{Ph}_2)][\text{PF}_6]_2$ (**3**). The red circle (●) denotes the NO stretch.

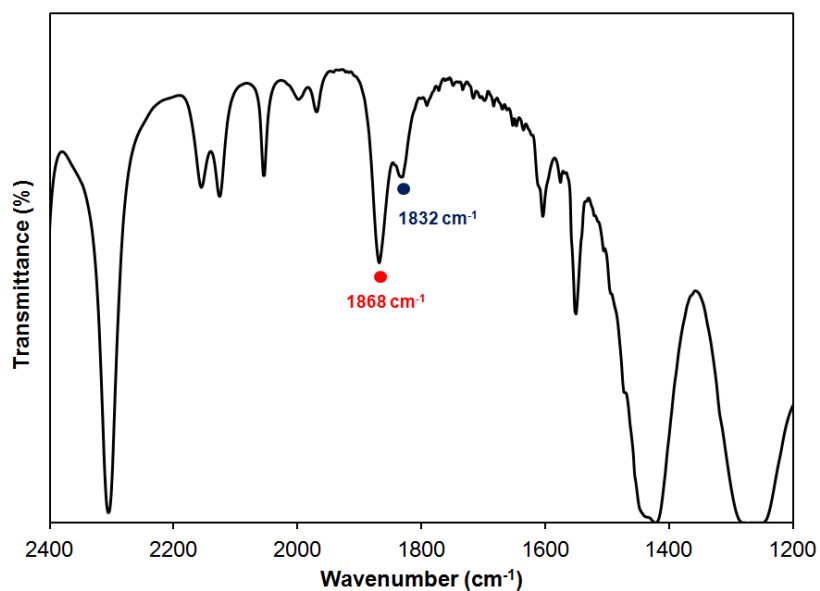


Figure S19. Solution phase IR spectrum (CH_2Cl_2 , 25 °C) of an isolated sample of $[\{(\text{NO})(\text{bipy})\text{Ni}\}_2(\mu\text{-S}_2\text{Ph}_2)][\text{PF}_6]_2$ (**3**). Significant dissociation occurs in solution. The red circle denotes the ν_{NO} of **2**, whereas, the navy circle denotes the ν_{NO} of **3**.

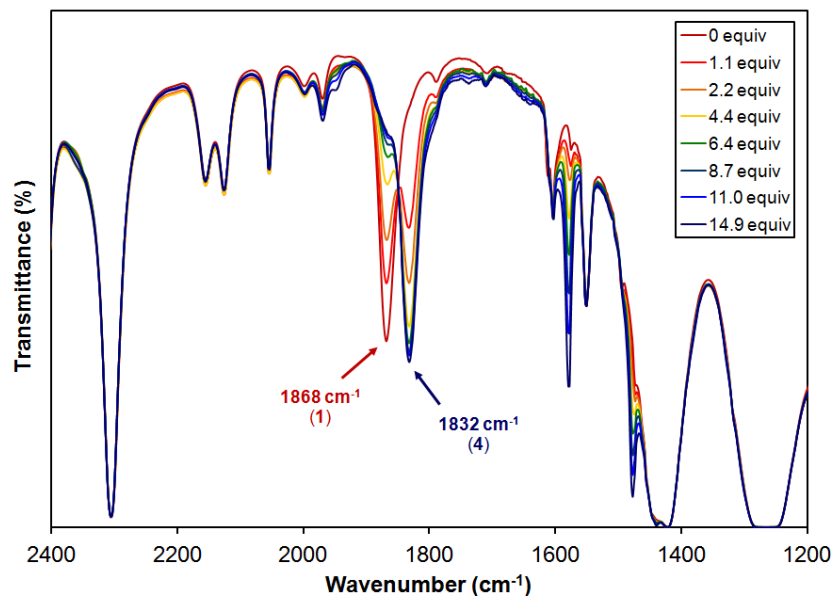


Figure S20. Monitoring the solution IR spectra (CH₂Cl₂, 25 °C) of **2** when titrated with Ph₂S₂. The number of equivalents is based on the stoichiometry of 0.5 Ph₂S₂ per Ni center.

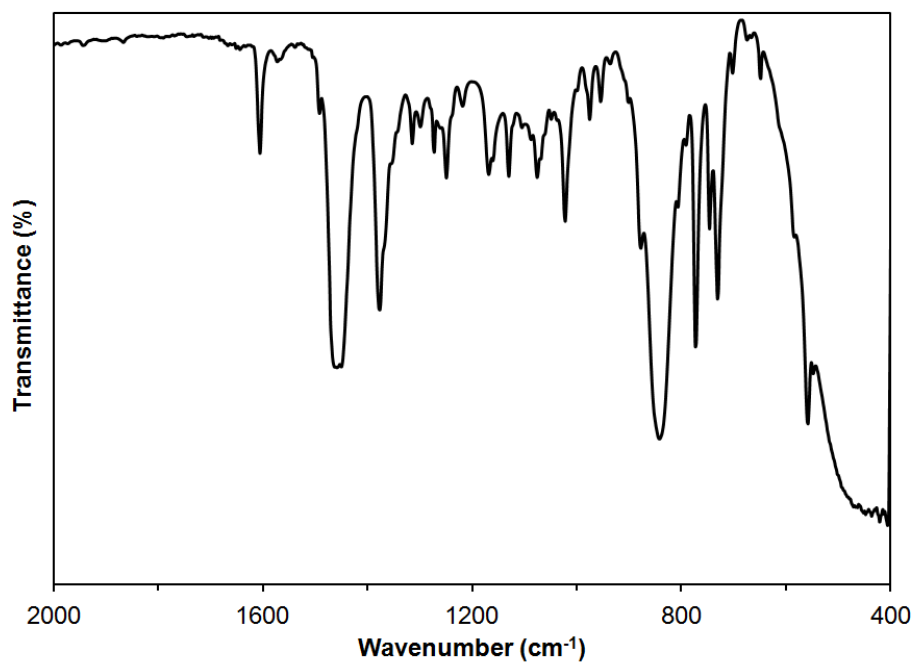


Figure S21. Solid state IR spectrum (Nujol mull) of [(bipy)Ni(TEMPO)][PF₆] (**4**).

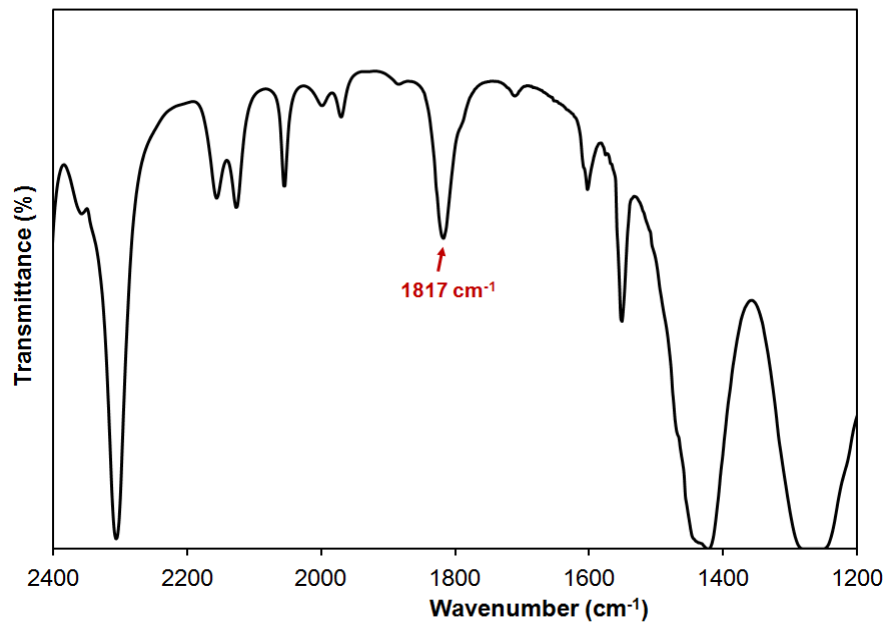


Figure S22. Solution IR spectrum (CH₂Cl₂, 25 °C) of [(bipy)NiNO(ONC₅H₅)] [PF₆] (**5**). The red arrow denotes the NO stretch.

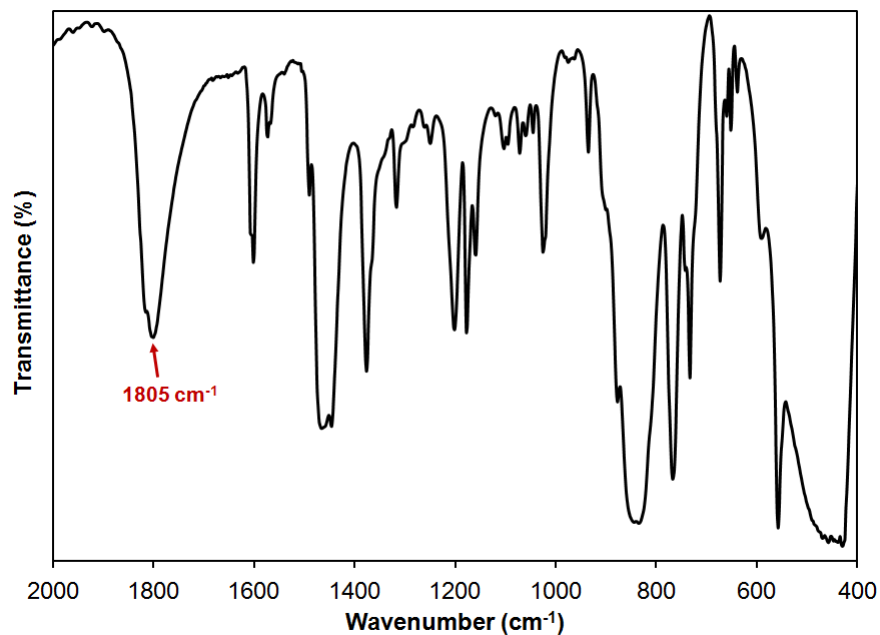


Figure S23. Solid-state IR spectrum (Nujol mull) of [(bipy)NiNO(ONC₅H₅)] [PF₆] (**5**). The red arrow denotes the NO stretch.

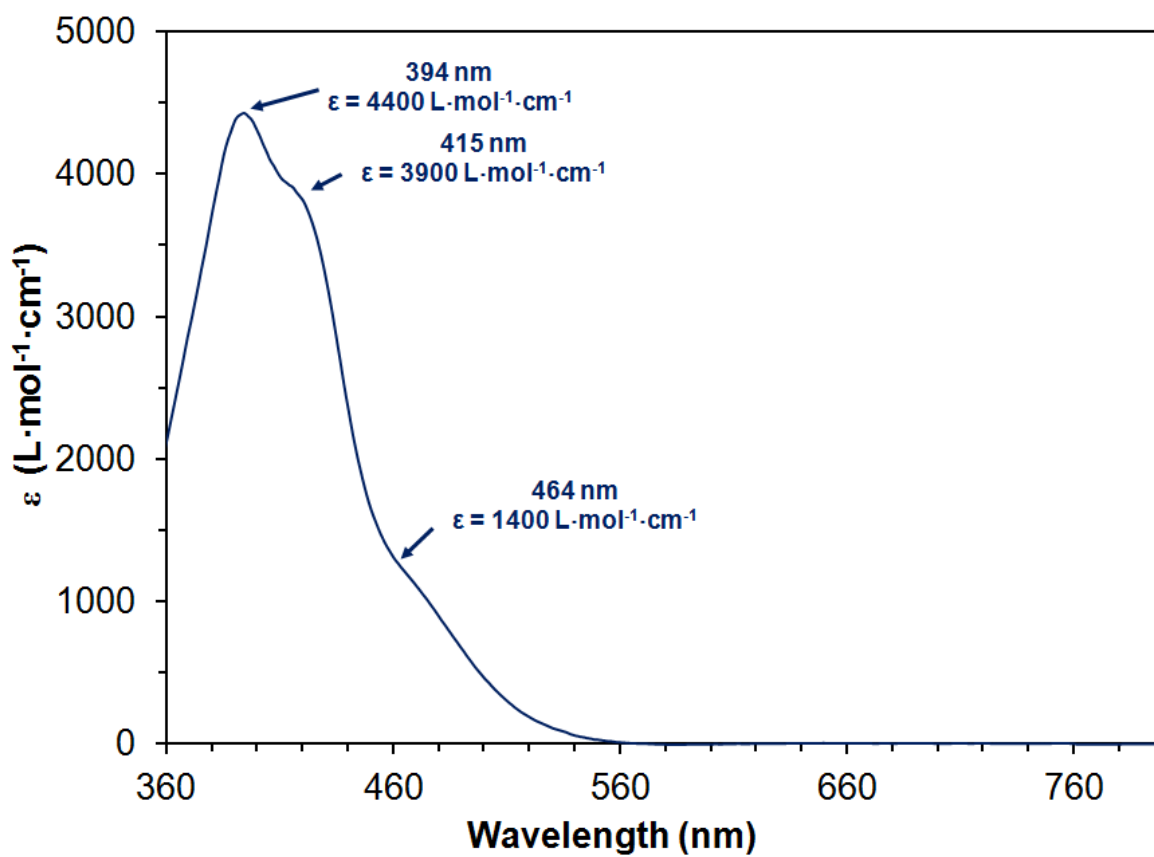


Figure S24. UV-vis spectrum (CH₂Cl₂, 25 °C, 0.45 mM) of [(bipy)Ni(TEMPO)][PF₆]₂ (**4**).

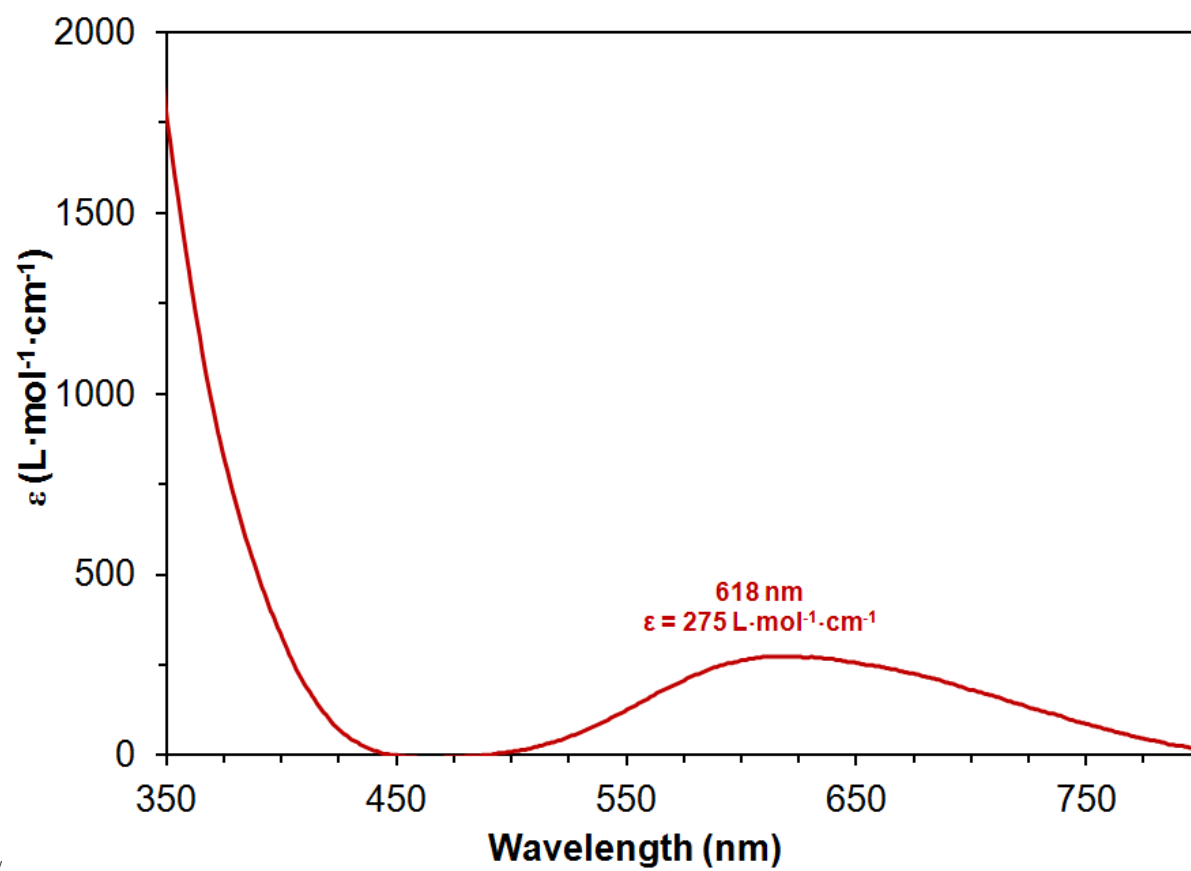


Figure S25. UV-vis spectra (CH₂Cl₂, 25 °C, 0.35 mM) of [(bipy)NiNO(ONC₅H₅)]PF₆ (5).

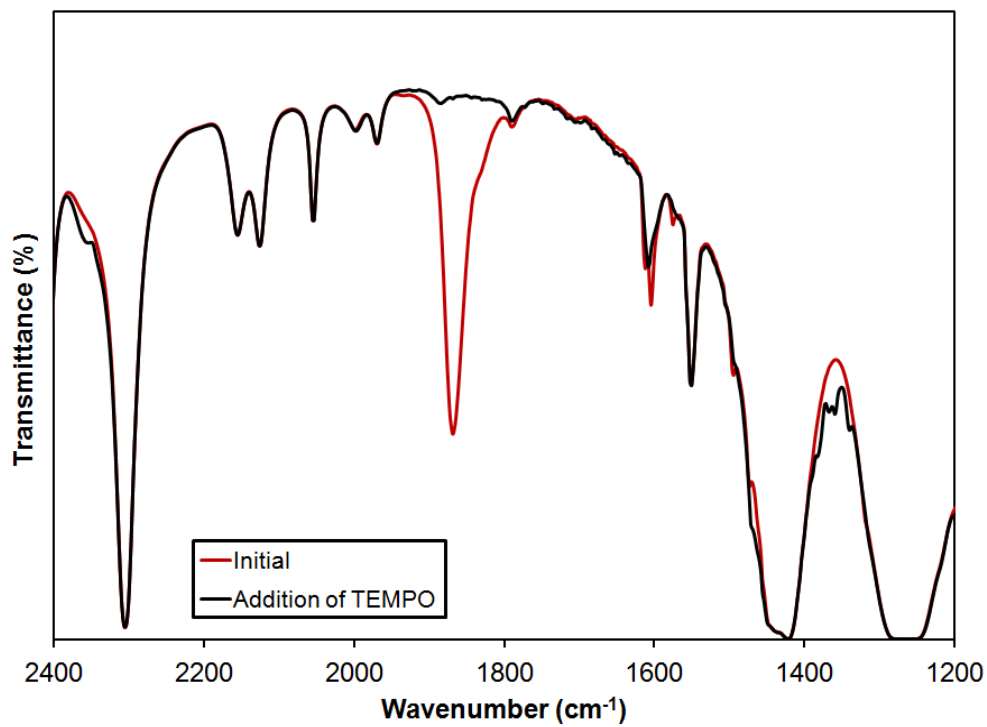


Figure S26. Solution IR spectra (CH₂Cl₂, 25 °C) of the reaction between **2** and TEMPO. The red trace is the initial spectrum of **2** and the black trace is after addition of TEMPO.

Gas Chromatography

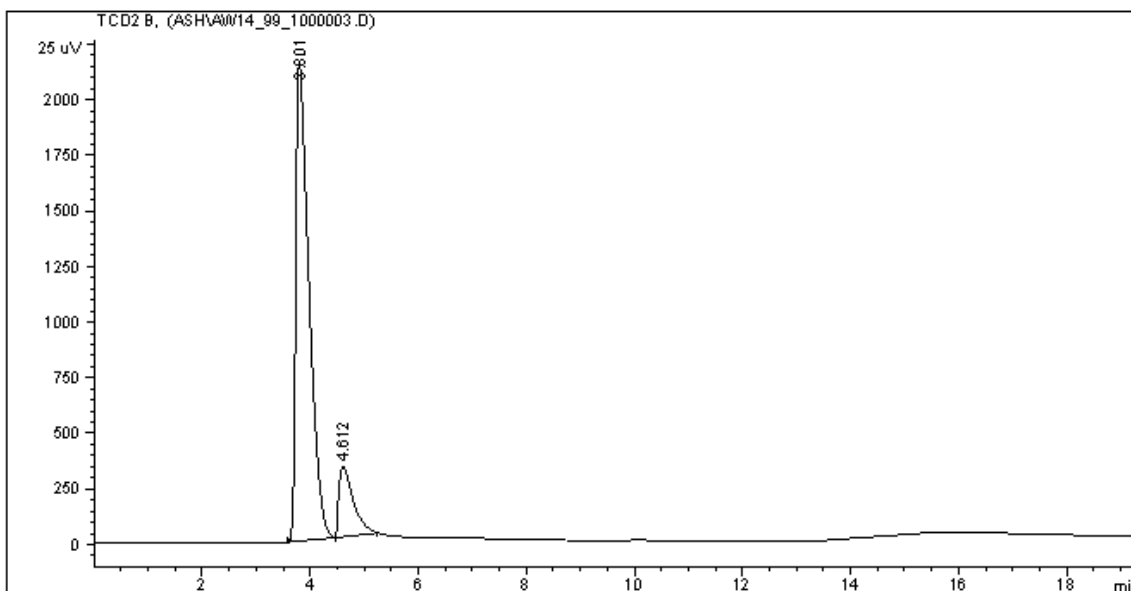


Figure S27. Gas chromatogram of the head space gases formed during the reaction between $[\text{Ni}(\text{NO})(\text{bipy})][\text{PF}_6]$ and TEMPO in CH_2Cl_2 . A 300 μL volume of the head space was sampled using a gas-tight Hamilton syringe and a GC trace was collected. The initial peak is N_2 (retention time, 3.8 min) and the second peak is NO (retention time, 4.6 min). N_2O is not observed as a product (retention time, 11.1 min).

Experimental Details: An airtight flask was charged with $[\text{Ni}(\text{NO})(\text{bipy})][\text{PF}_6]$ (68 mg, 0.17 mmol) and CH_2Cl_2 (1.22 mL). TEMPO (38 mg, 0.24 mmol) was injected as a CH_2Cl_2 solution (0.97 mL) in to the reaction flask through a rubber septum. After 30 minutes, a 300 μL volume of the head space was sampled using a gas-tight Hamilton syringe.

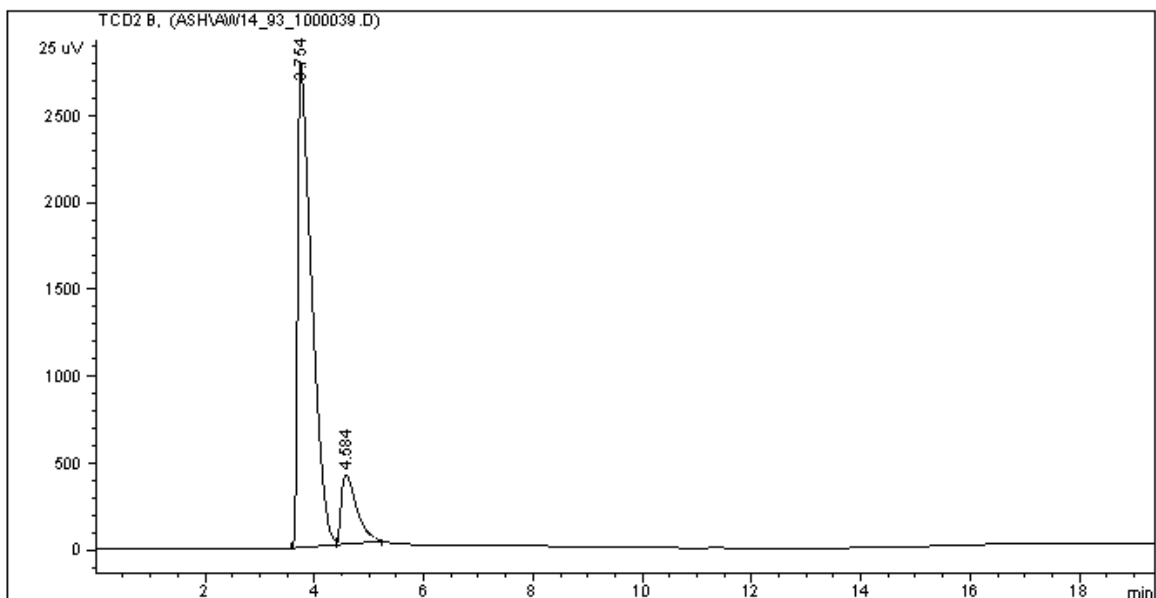


Figure S28. Gas chromatogram of the head space gases formed during the reaction between $[\text{Ni}(\text{NO})(\text{bipy})][\text{PF}_6]$ and $[\text{NO}][\text{PF}_6]$ in MeCN. A 300 μL volume of the head space was sampled using a gas-tight Hamilton syringe and a GC trace was collected. The initial peak is N_2 (retention time, 3.8 min) and the second peak is NO (retention time, 4.6 min). N_2O is not observed as a product (retention time, 11.1 min).

Experimental Details: An airtight flask was charged with $[\text{Ni}(\text{NO})(\text{bipy})][\text{PF}_6]$ (38 mg, 0.097 mmol) and CH_3CN (0.73 mL). $[\text{NO}][\text{PF}_6]$ (38 mg, 0.24 mmol) was injected as a CH_3CN solution (0.42 mL) into the reaction flask through a rubber septum. Rapid gas evolution was observed and the solution color turned a pale purple. After 30 minutes, a 300 μL volume of the head space was sampled using a gas-tight Hamilton syringe.

Reactivity Studies

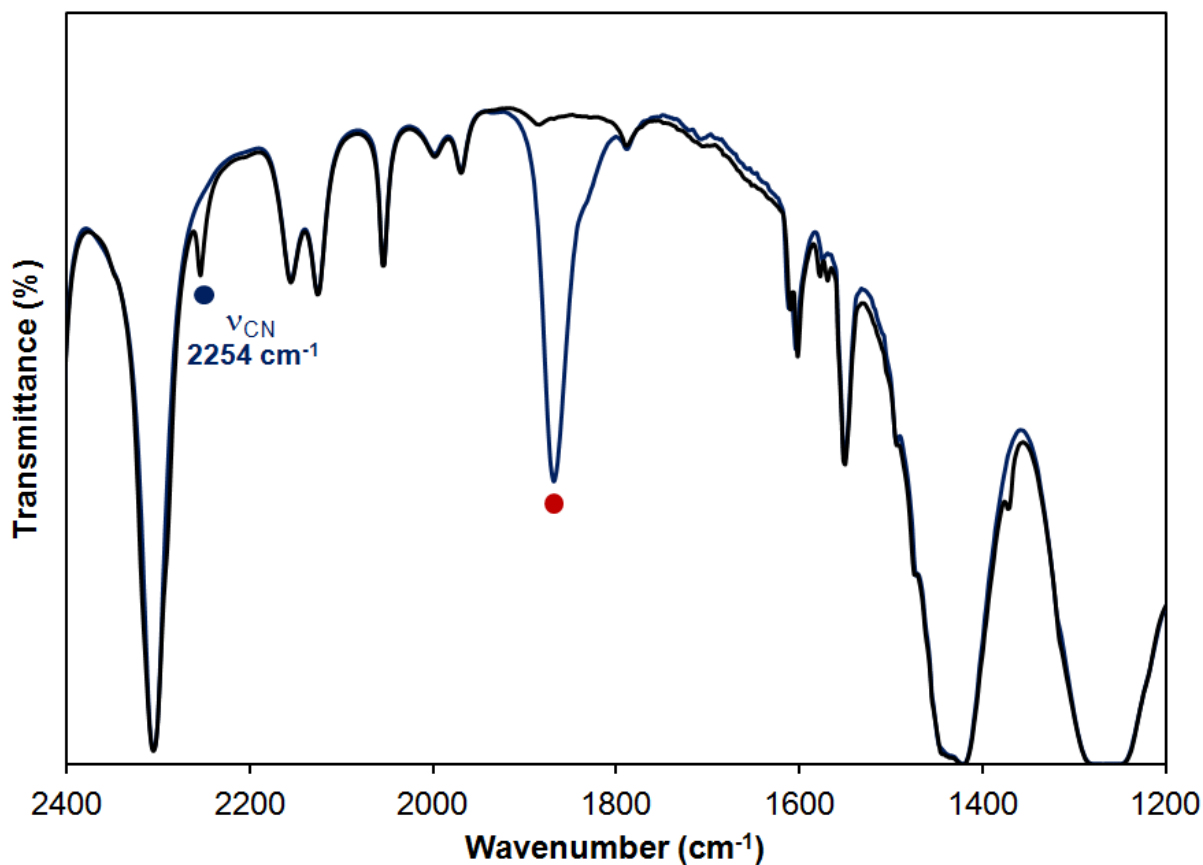


Figure S29. Solution IR spectrum (CH₂Cl₂, 25 °C) of complex **2** before and after the addition of [NO][PF₆], and subsequent addition of MeCN. The blue trace is the initial spectrum of complex **2**. The red circle denotes the NO stretch for **2**. The black trace is this solution 15 minutes after addition of 4.5 equiv of MeCN and [NO][PF₆]. The dark blue circle denotes a CN stretch of MeCN.

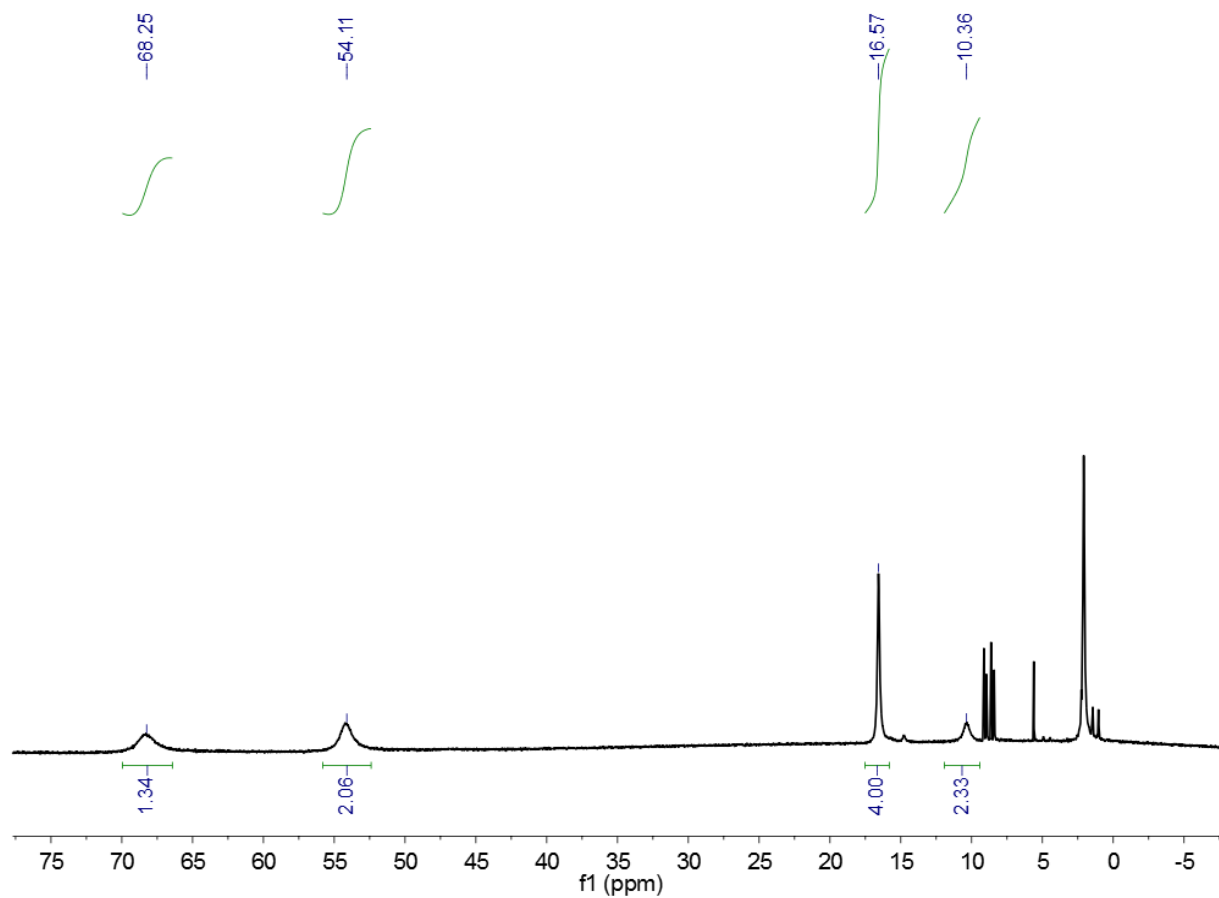


Figure S30. ^1H NMR spectrum (CD_3CN , 22 °C 400 MHz) of the in situ reaction mixture between complex **2** and $[\text{NO}][\text{PF}_6]$.

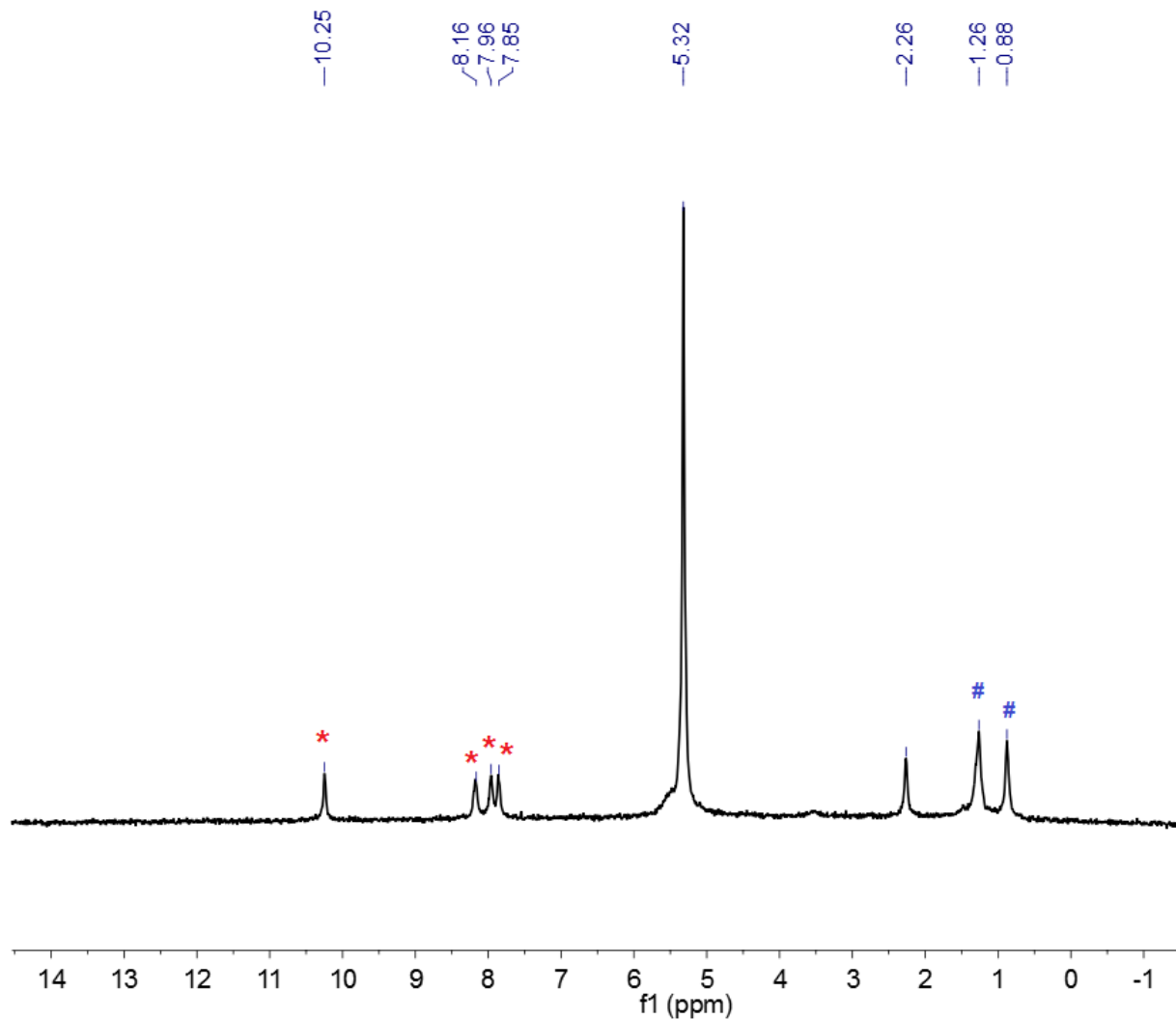


Figure S31. ^1H NMR spectrum (CD_2Cl_2 , 400 MHz, 22 $^\circ\text{C}$) of $[\text{Ni}(\text{NO})(\text{bipy})][\text{PF}_6]$ and AgPF_6 after 24 hours. The intensity of the resonances for **2**, denoted by the red asterisks (*), has significantly decreased. A large amount of precipitate, including a silver mirror, has formed inside the NMR tube. The blue hashes (#) are assigned to a hexane impurity.

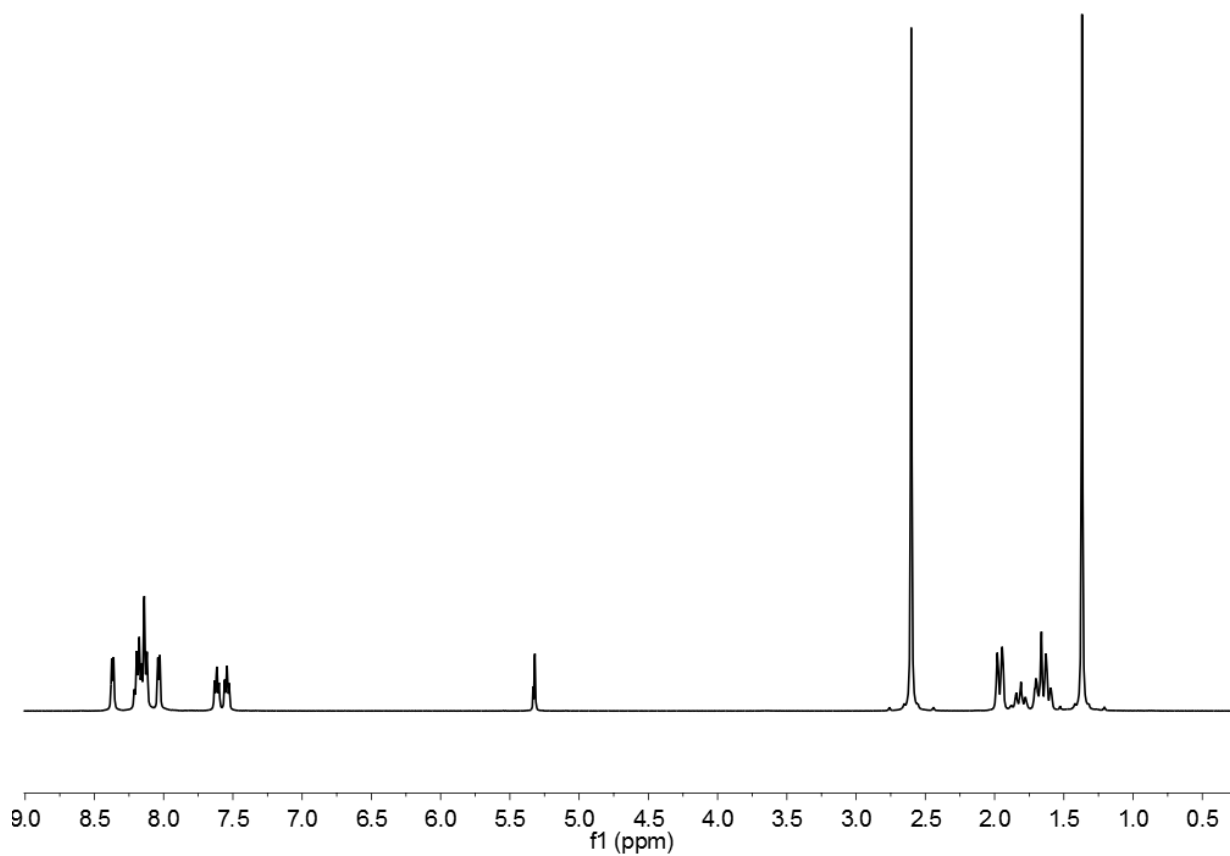


Figure S32. ¹H NMR spectrum (CD₂Cl₂, 400 MHz, 22 °C) of the reaction between **2** and TEMPO. There is clean conversion to **4**.

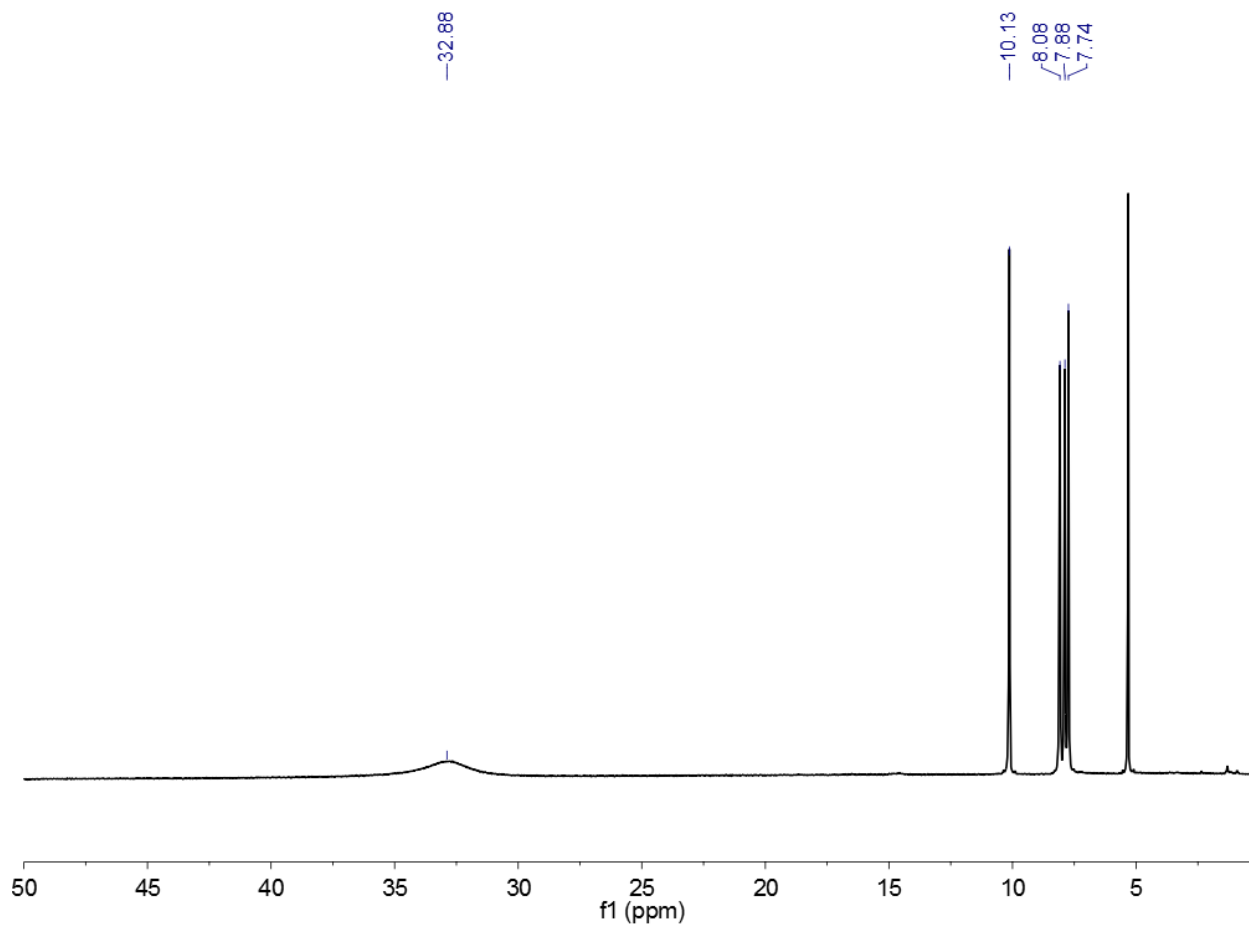


Figure S33. ¹H NMR spectrum (CD₂Cl₂, 400 MHz, 22 °C) of [Ni(NO)(bipy)][PF₆] and [Fc][PF₆] after 24 hours. The intensity of the resonances for **2** remain unchanged upon addition of [Fc][PF₆].

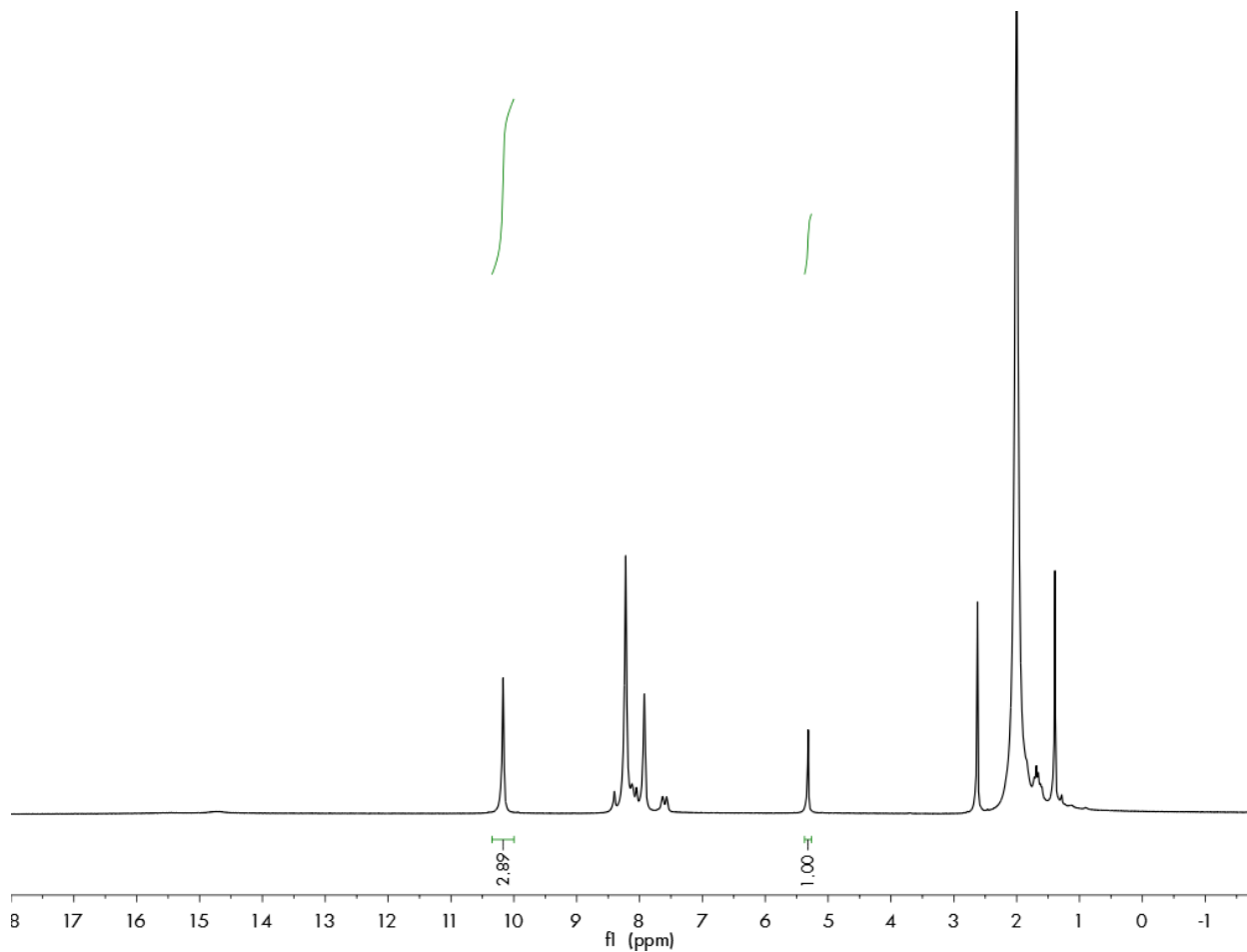


Figure S34. ¹H NMR spectrum (CD₂Cl₂, 400 MHz, 22 °C) of the reaction between TEMPO and [Ni(NO)(bipy)][PF₆] in the presence of 5 equiv of MeCN after 24 hours. After 24 hours, the reaction is approximately 25% complete. The unreacted TEMPO is not observed in the spectrum as its resonances are paramagnetically broadened.

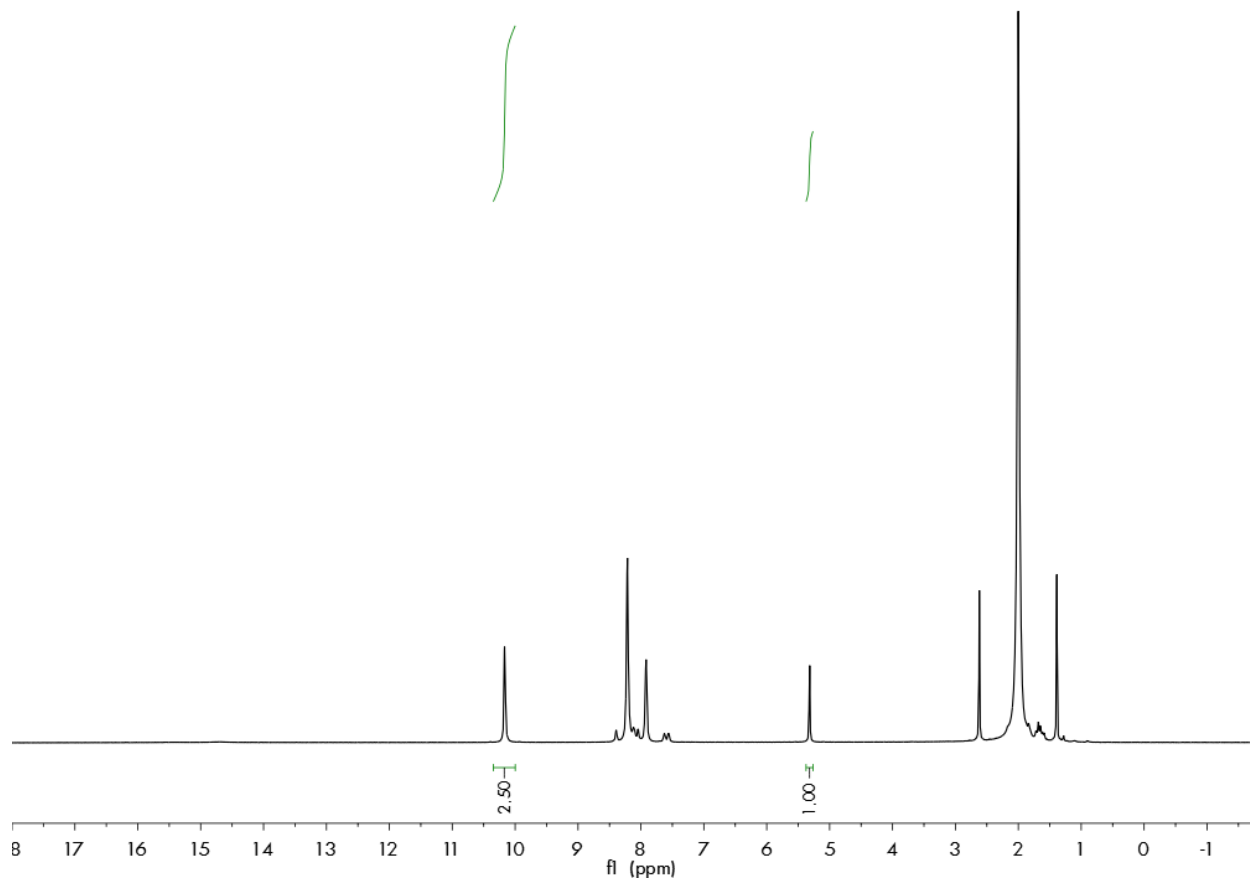


Figure S35. ¹H NMR spectrum (CD₂Cl₂, 400 MHz, 22 °C) of the reaction between TEMPO and [Ni(NO)(bipy)][PF₆] in the presence of 5 equiv of MeCN after 72 hours. After 72 hours, the reaction is approximately 35% complete. The unreacted TEMPO is not observed in the spectrum as its resonances are paramagnetically broadened.

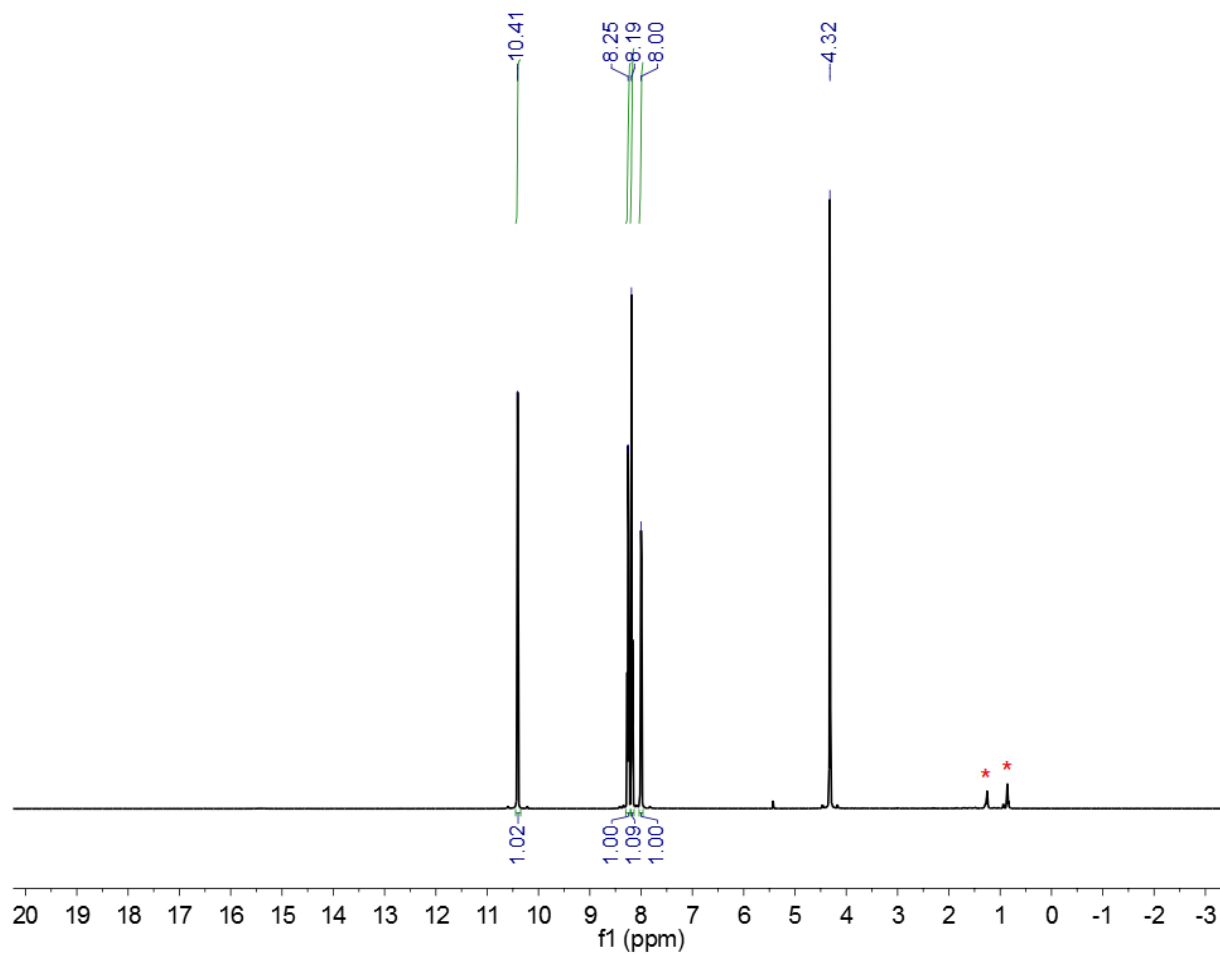


Figure S36. ^1H NMR spectrum (CD_3NO_2 , 500 MHz, 22 °C) of **2** before heating. The red asterisks denote a hexane impurity.

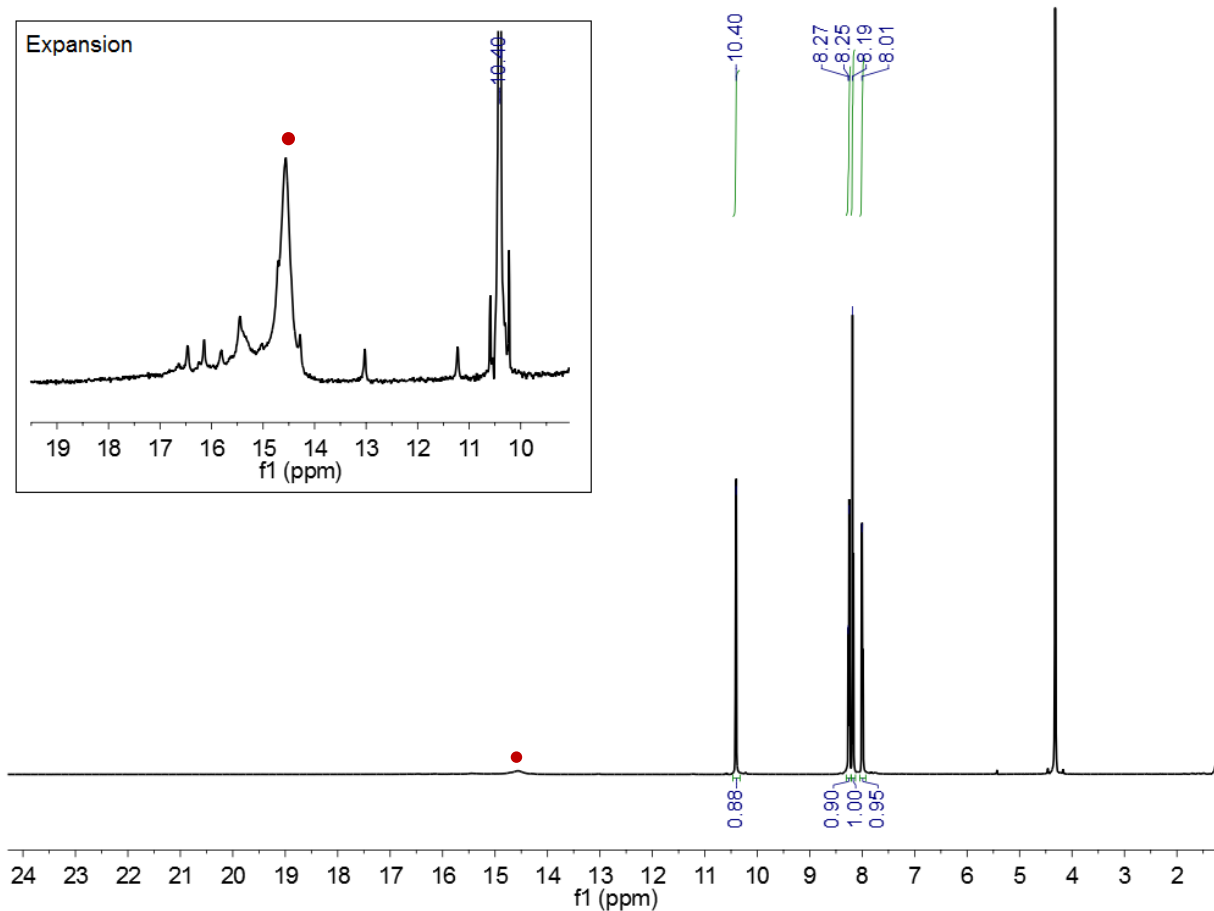


Figure S37. ^1H NMR spectrum (CD_3NO_2 , 500 MHz, 22 °C) of **2** after heating at 90 °C for 24 h. The inset shows a number of minor resonances that are the result of decomposition. The red circle denotes a resonance assigned to $[\text{Ni}(\text{bipy})_3][\text{PF}_6]_2$.

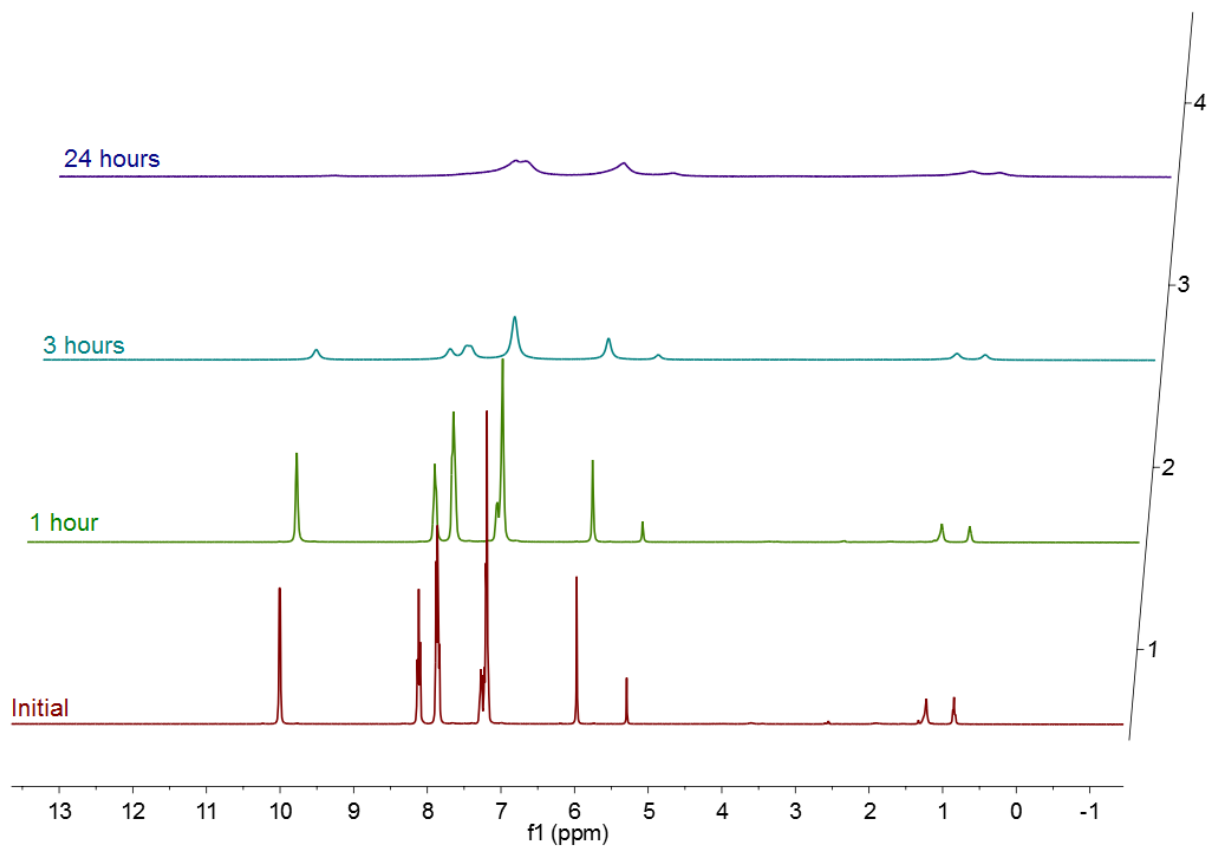


Figure S38. ^1H NMR spectra ($1,1,2,2\text{-C}_2\text{Cl}_4\text{D}_2$, 400 MHz, 22 °C) of the thermolysis of **3** at 60 °C recorded at intervals over the course of 24 hrs. A green precipitate is formed over the course of this reaction and there are no signals observed outside of the spectral region shown above.

Electrochemistry

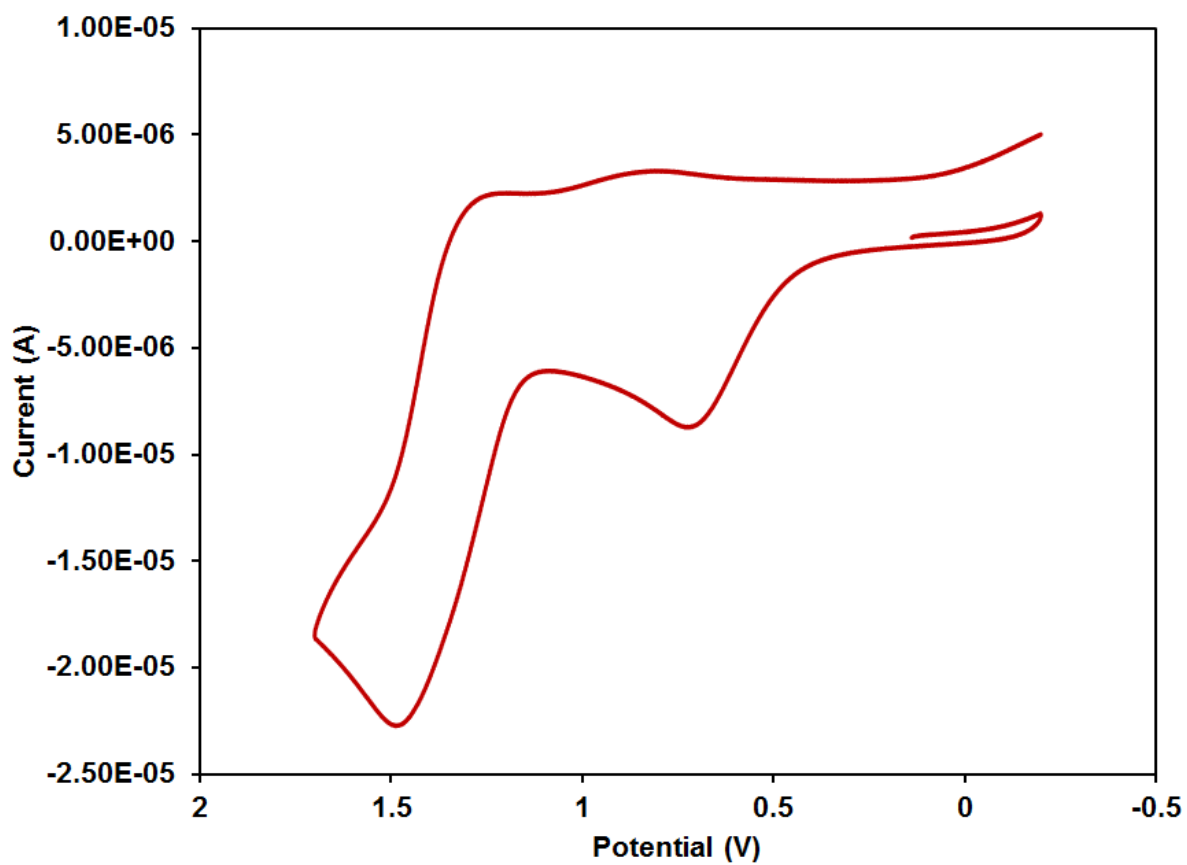


Figure S39. Room temperature cyclic voltammogram of **2** in MeCN vs. $[\text{Cp}_2\text{Fe}]^{0+}$. (Scan rate 0.2 V/s; 0.1 M $[\text{Bu}_4\text{N}][\text{PF}_6]$ as supporting electrolyte).

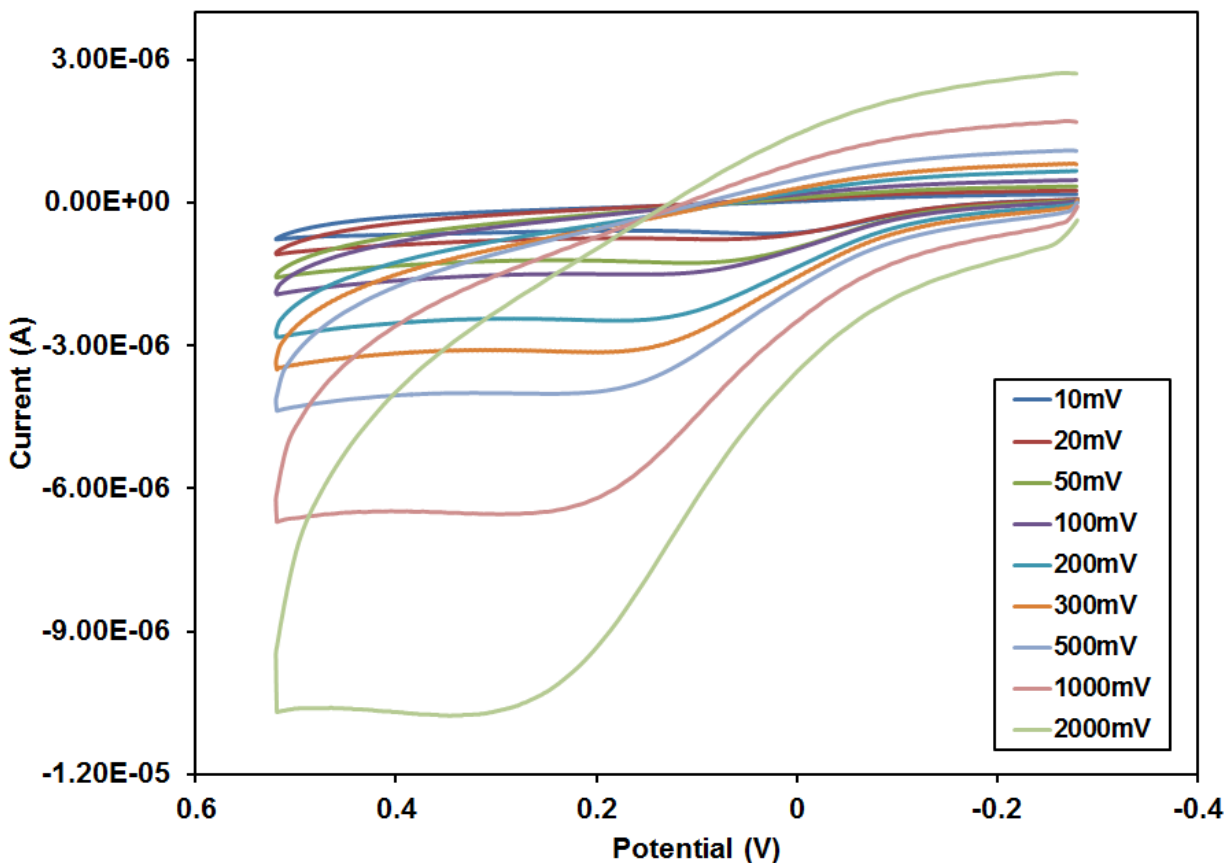


Figure S40. Partial room temperature cyclic voltammogram of **2** in MeCN vs. $[\text{Cp}_2\text{Fe}]^{0/+}$ (0.1 M $[\text{Bu}_4\text{N}][\text{PF}_6]$ as supporting electrolyte).

Table S2. Electrochemical data of complex **2** in MeCN vs $[\text{Cp}_2\text{Fe}]^{0/+}$.

Oxidation Feature	Scan Rate V/s	$E_{p,a}$, V
	10	0.032
	25	0.051
	50	0.077
	100	0.106
	200	0.144
	300	0.164
	500	0.190
	1000	0.231
	2000	0.287

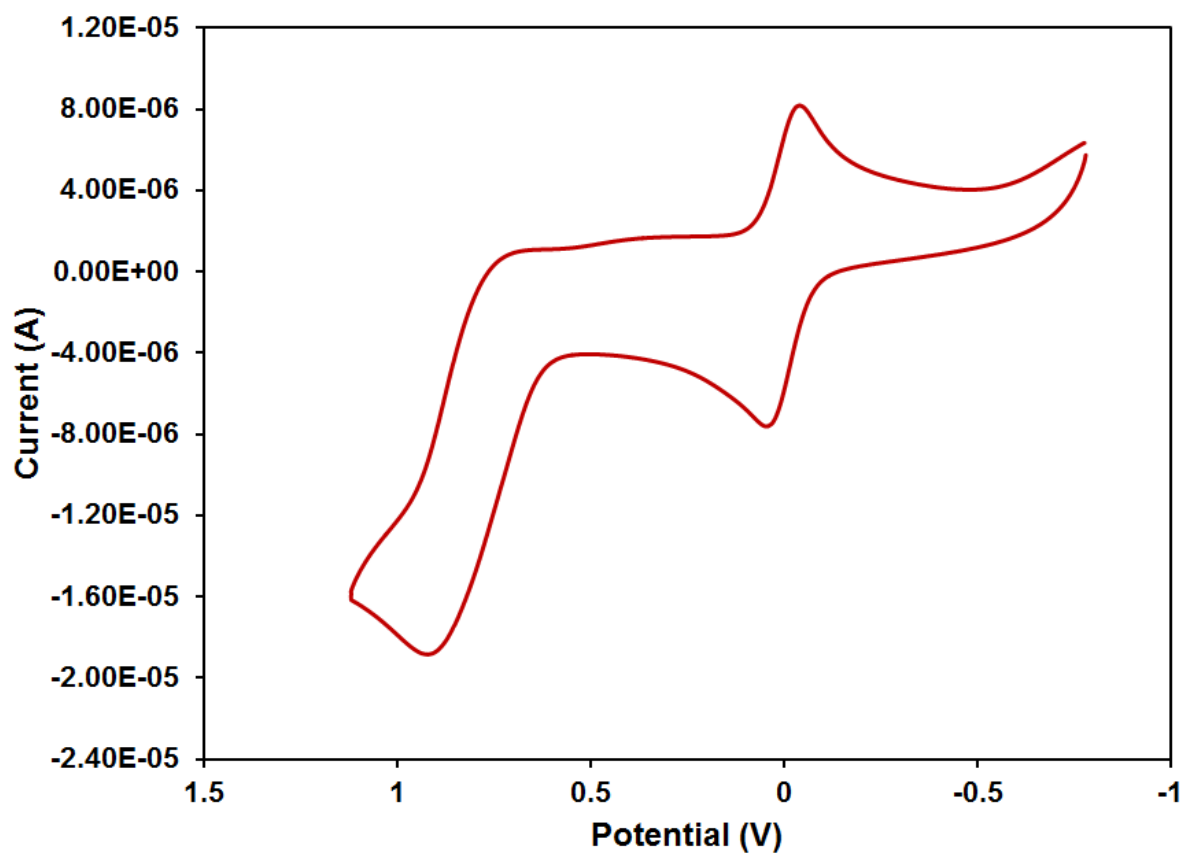


Figure S41. Room temperature cyclic voltammogram of **2** and ferrocene in MeCN vs. $[\text{Cp}_2\text{Fe}]^{0/+}$ (Scan rate 0.2 V/s; 0.1 M $[\text{Bu}_4\text{N}][\text{PF}_6]$ as supporting electrolyte).

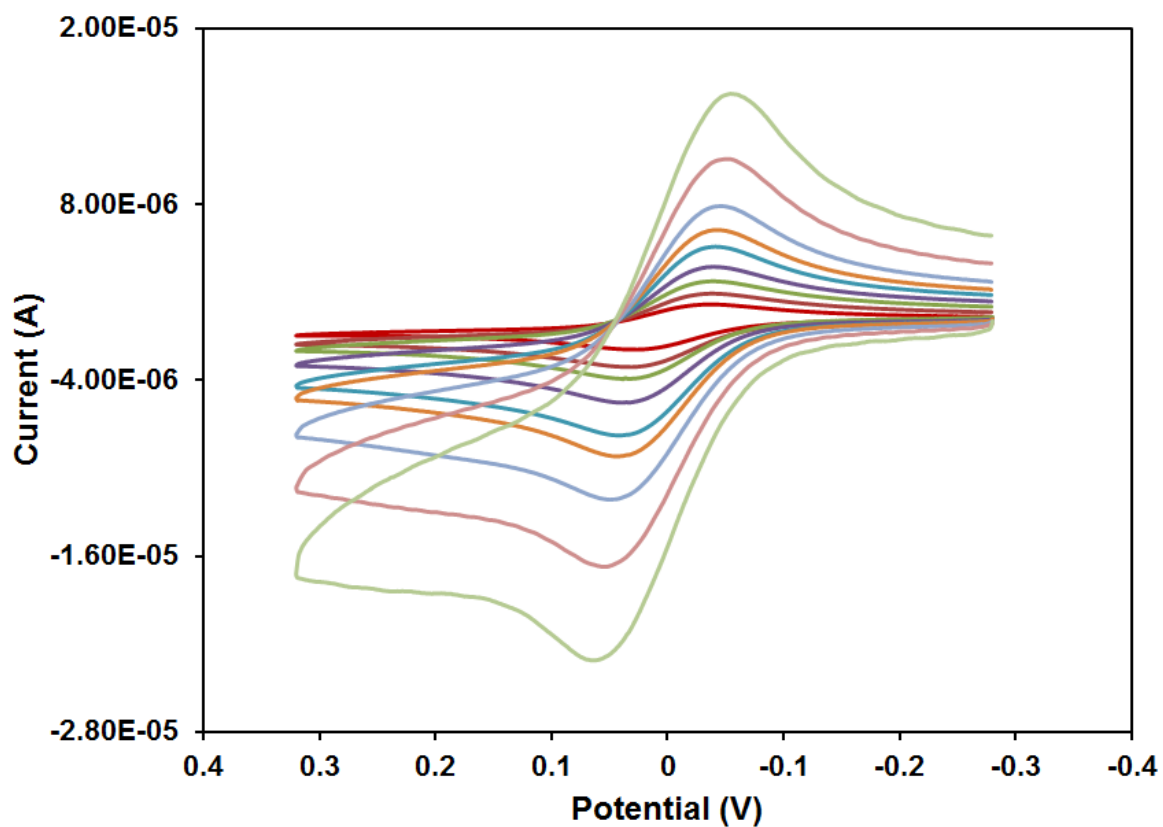


Figure S42. Room temperature cyclic voltammogram of ferrocene and **2** in MeCN vs. $[\text{Cp}_2\text{Fe}]^{0+}$ (0.1 M $[\text{Bu}_4\text{N}][\text{PF}_6]$ as supporting electrolyte).

Table S3. Electrochemical data of ferrocene in MeCN vs. $[\text{Cp}_2\text{Fe}]^{0+}$.

Ferrocene	Scan Rate V/s	$E_{p,a}$, V	$\Delta E_{p,c}$ V	Δ	$i_{p,c}/i_{p,a}$
	10	0.031	-0.037	0.068	0.83
	25	0.033	-0.039	0.072	0.77
	50	0.038	-0.039	0.077	0.84
	100	0.039	-0.038	0.077	0.85
	200	0.041	-0.042	0.083	0.85
	300	0.043	-0.042	0.085	0.86
	500	0.050	-0.047	0.097	0.83
	1000	0.054	-0.052	0.106	0.82
	2000	0.064	-0.054	0.118	0.81

References

- (1) Gutmann, V. *Coord. Chem. Rev.* **1976**, *18*, 225-255.